

Report 23: State-level tracking of COVID-19 in the United States

H Juliette T Unwin*, Swapnil Mishra*², Valerie C Bradley*, Axel Gandy*, Michaela A C Vollmer, Thomas Mellan, Helen Coupland, Kylie Ainslie, Charlie Whittaker, Jonathan Ish-Horowicz, Sarah Filippi, Xiaoyue Xi, Melodie Monod, Oliver Ratmann, Michael Hutchinson, Fabian Valka, Harrison Zhu, Iwona Hawryluk, Philip Milton, Marc Baguelin, Adhiratha Boonyasiri, Nick Brazeau, Lorenzo Cattarino, Giovanni Charles, Laura V Cooper, Zulma Cucunuba, Gina Cuomo-Dannenburg, Bimandra Djaafara, Ilaria Dorigatti, Oliver J Eales, Jeff Eaton, Sabine van Elsland, Richard FitzJohn, Katy Gaythorpe, William Green, Timothy Hallett, Wes Hinsley, Natsuko Imai, Ben Jeffrey, Edward Knock, Daniel Laydon, John Lees, Gemma Nedjati-Gilani, Pierre Nouvellet, Lucy Okell, Alison Ower, Kris V Parag, Igor Siveroni, Hayley A Thompson, Robert Verity, Patrick Walker, Caroline Walters, Yuanrong Wang, Oliver J Watson, Lilith Whittles, Azra Ghani, Neil M Ferguson, Steven Riley, Christl A. Donnelly, Samir Bhatt^{1,*} and Seth Flaxman*

Department of Infectious Disease Epidemiology, Imperial College London

Department of Mathematics, Imperial College London

WHO Collaborating Centre for Infectious Disease Modelling

MRC Centre for Global Infectious Disease Analytics

Abdul Latif Jameel Institute for Disease and Emergency Analytics, Imperial College London

Department of Statistics, University of Oxford

*Contributed equally.

¹Correspondence: s.bhatt@imperial.ac.uk

²Methodological correspondence: s.mishra@imperial.ac.uk

SUGGESTED CITATION

H Juliette T Unwin, Swapnil Mishra, Valerie C Bradley *et al.* Report 23: State-level tracking of COVID-19 in the United States (21-05-2020), doi: <https://doi.org/10.25561/79231>.



This work is licensed under a Creative Commons Attribution-NonCommercial-NoDerivatives 4.0 International License.

Summary

As of 20 May 2020, the US Centers for Disease Control and Prevention reported 91,664 confirmed or probable COVID-19-related deaths, more than twice the number of deaths reported in the next most severely impacted country. In order to control the spread of the epidemic and prevent health care systems from being overwhelmed, US states have implemented a suite of non-pharmaceutical interventions (NPIs), including “stay-at-home” orders, bans on gatherings, and business and school closures.

We model the epidemics in the US at the state-level, using publicly available death data within a Bayesian hierarchical semi-mechanistic framework. For each state, we estimate the time-varying reproduction number (the average number of secondary infections caused by an infected person), the number of individuals that have been infected and the number of individuals that are currently infectious. We use changes in mobility as a proxy for the impact that NPIs and other behaviour changes have on the rate of transmission of SARS-CoV-2. We project the impact of future increases in mobility, assuming that the relationship between mobility and disease transmission remains constant. We do not address the potential effect of additional behavioural changes or interventions, such as increased mask-wearing or testing and tracing strategies.

Nationally, our estimates show that the percentage of individuals that have been infected is 4.1% [3.7%-4.5%], with wide variation between states. For all states, even for the worst affected states, we estimate that less than a quarter of the population has been infected; in New York, for example, we estimate that 16.6% [12.8%-21.6%] of individuals have been infected to date. Our attack rates for New York are in line with those from recent serological studies [1] broadly supporting our modelling choices.

There is variation in the initial reproduction number, which is likely due to a range of factors; we find a strong association between the initial reproduction number with both population density (measured at the state level) and the chronological date when 10 cumulative deaths occurred (a crude estimate of the date of locally sustained transmission).

Our estimates suggest that the epidemic is not under control in much of the US: as of 17 May 2020, the reproduction number is above the critical threshold (1.0) in 24 [95% CI: 20-30] states. Higher reproduction numbers are geographically clustered in the South and Midwest, where epidemics are still developing, while we estimate lower reproduction numbers in states that have already suffered high COVID-19 mortality (such as the Northeast). These estimates suggest that caution must be taken in loosening current restrictions if effective additional measures are not put in place.

We predict that increased mobility following relaxation of social distancing will lead to resurgence of transmission, keeping all else constant. We predict that deaths over the next two-month period could exceed current cumulative deaths by greater than two-fold, *if* the relationship between mobility and transmission remains unchanged. Our results suggest that factors modulating transmission such as rapid testing, contact tracing and behavioural precautions are crucial to offset the rise of transmission associated with loosening of social distancing.

Overall, we show that while all US states have substantially reduced their reproduction numbers, we find no evidence that any state is approaching herd immunity or that its epidemic is close to over.

We invite scientific peer reviews here: <https://openreview.net/group?id=Agora/COVID-19>

1 Introduction

The first death caused by COVID-19 in the United States is currently believed to have occurred in Santa Clara, California on the 6th February [2]. In April 2020, the number of deaths attributed to COVID-19 in the United States (US) surpassed that of Italy [3]. Throughout March 2020, US state governments implemented a variety of non-pharmaceutical interventions (NPIs), such as school closures and stay-at-home orders, to limit the spread of SARS-CoV-2 and help maintain the capacity of health systems to treat as many severe cases of COVID-19 as possible. Courtemanche *et al.* [4] use an event-study model to determine that such NPIs were successful in reducing the growth rate of COVID-19 cases across US counties. We similarly seek to estimate the impact of NPIs on COVID-19 transmission, but do so with a semi-mechanistic Bayesian model that reflects the underlying process of disease transmission and relies on mobility data released by companies such as Google [5]. Mobility measures reveal stark changes in behaviour following large-scale government interventions, with individuals spending more time at home and correspondingly less time at work, at leisure centres, shopping, and on public transit. Some state governments, like the Colorado Department of Public Health, have already begun to use similar mobility data to adjust guidelines over social distancing [6]. As more and more states ease the stringency of their NPIs, future policy decisions will rely on the interaction between mobility and NPIs and their subsequent impact on transmission.

In a previous report [7], we introduced a new Bayesian statistical framework for estimating the rate of transmission and attack rates for COVID-19. Our approach infers the time-varying reproduction number, R_t , which measures transmission intensity. We calculate the number of new infections through combining previous infections with the generation interval (the distribution of times between infections). The number of deaths is then a function of the number of infections and the infection fatality rate (IFR). We estimate the posterior probability of our parameters given the observed data, while incorporating prior uncertainty. This makes our approach empirically driven while incorporating as many sources of uncertainty as possible. In this report, similar to [8, 9], we adapt our original framework to model transmission in the US at the state level. In our formulation we parameterise R_t as a function of several mobility types. Our parameterisation of R_t makes the explicit assumption that changes in transmission are reflected through mobility. While we do attempt to account for residual variation, we note that transmission will also be influenced by additional factors and some of these are confounded causally with mobility. We utilise partial pooling of parameters, where information is shared across all states to leverage as much signal as possible, but individual effects are also included for state- and region-specific idiosyncrasies. Our partial pooling model requires only one state to provide a signal for the impact of mobility, and then this effect is shared across all states. While this sharing can potentially lead to initial over or under estimation effect sizes, it also means that a consistent signal for all states can be estimated before that signal is presented in an individual states with little data.

We infer plausible upper and lower bounds (Bayesian credible interval summaries of our posterior distribution) of the total population that have been infected by COVID-19 (also called the cumulative attack rate or attack rate). We also estimate the effective number of individuals currently infectious given our generation distribution. We investigate how the reproduction number has changed over time and study the heterogeneity in starting and ending rates by state, date, and population density. We assess whether there is evidence that changes in mobility have so far been successful at reducing R_t to less than 1. To assess the risk of resurgence when interventions are eased, we use simple scenarios of increased mobility and simulate forwards in time. From these simulations we study how sensitive individual states are

to resurgence, and the plausible magnitude of this resurgence.

Details of the data sources and a technical description of our model and are found in Sections 4 and 5 respectively. General limitations of our approach are presented below in the conclusions.

2 Results

2.1 Mobility trends, interventions and effect sizes

Mobility data provide a proxy for the behavioural changes that occur in response to non-pharmaceutical interventions. Figure 1 shows trends in mobility for the 50 states and the District of Columbia (see Section 4 for a description of the mobility dimensions). Regions are based on US Census Divisions, modified to account for coordination between groups of state governments [10]. These trends are relative to a state-dependent baseline, which was calculated shortly before the COVID-19 epidemic. For example, a value of -20% in the transit station trend means that individuals, on average, are visiting and spending 20% less time in transit hubs than before the epidemic. In Figure 1, we overlay the timing of two major state-wide NPIs (stay at home and emergency decree) (see [11] for details). We also note intuitive changes in mobility such as the spike on 11th and 12th April for Easter. In our model, we use the time spent at one's residence and the average of time spent at grocery stores, pharmacies, recreation centres, and workplaces. For states in which the 2018 American Community Survey reports that more than 20% of the working population commutes on public transportation, we also use the time spent at transit hubs (including gas stations etc.) [12].

To justify the use of mobility as a proxy for behaviour, we regress average mobility against the timings of major NPIs (represented as step functions). The median correlation between the observed average mobility and the linear predictions from NPIs was approximately 89% (see Appendix A). We observed reduced correlation when lagging (forward and backwards) the timing of NPIs suggesting immediate impact on mobility. We make no explicit causal link between NPIs and mobility, however, this relationship is plausibly causally linked but is confounded by other factors.

The mobility trends data suggests that the United States' national focus on the New York epidemic may have led to substantial changes in mobility in nearby states, like Connecticut, prior to any mandated interventions in those states. This observation adds support to the hypothesis that mobility can act as a suitable proxy for the changes in behaviour induced by the implementation of the major NPIs. In further corroboration, a poll conducted by Morning Consult/Politico on 26th March 2020 found that 81% of respondents agreed that "Americans should continue to social distance for as long as is needed to curb the spread of coronavirus, even if it means continued damage to the economy" [13]. While support for strong social distancing has since eroded slightly (70% agree in the same poll conducted later on 10 May 2020), the overall high support for social distancing suggests strong compliance with NPIs, and that the changes to mobility that we observe over the same time period are driven by adherence to those policy recommendations. However, we note that mobility alone cannot capture all the heterogeneity in transmission risk. In particular, it cannot capture the impact of case-based interventions (such as testing and tracing). To account for this residual variation missed by mobility we use a second-order, weekly, autoregressive process. This autoregressive process is an additional term in our parametric equation for R_t and accounts for residual noise by capturing a correlation structure where current R_t is correlated with previous weeks R_t (see Figures 12).

Figure 2 shows the average global effect sizes for the mobility types used in our model. Estimates for the regional and state-level effect sizes are included in Appendix B. We find that increased time spent in residences reduces transmission by 54.3% [17.8% - 80.8%], and that decreases in overall average mobility reduced transmission by 62.7% [43.1% - 74.5%]. These two effects are likely related - as people spend less time in public spaces, captured by our average mobility metric, they conversely spend more time at home. Overall, this decreases the number of people with whom the average individual comes into contact, thus slowing transmission, even if more time at home may increase transmission within a single residence. We find time spent in transit hubs does not have a significant effect on transmission. The impact of transit mobility is in contrast to what we observed in Italy [8], and likely reflects higher reliance on cars and less use of public transit in the US than Europe [14].

The learnt random effects from the autoregressive process are shown in Appendix C. These results show that mobility explains most of the changes in transmission in places without advanced epidemics, as evidenced by the flat residual variation. However, for regions with advanced epidemics, such as New York or New Jersey, there is evidence of additional decreases in transmission that cannot be explained by mobility alone. These may capture the impact of other control measures, such as increased testing, as well as behavioural responses not captured by mobility, like increased mask-wearing and hand-washing.

2.2 Impact of interventions on reproduction numbers

We estimate a national average initial reproduction number ($R_{t=0}$) of 2.2 [0.3 Montana - 5.0 New York] and find that, similar to influenza transmission in cities (see Dalziel *et al.* [15]), $R_{t=0}$ is correlated with population density (Figure 3)¹. Dalziel *et al.* hypothesize that more personal contact occurs in more densely populated areas, thus resulting in a larger $R_{t=0}$.

$R_{t=0}$ is also negatively correlated with when a state observed cumulative 10 deaths (Figure 3). This negative correlation implies that states began locally sustained transmission later had a lower $R_{t=0}$. A possible hypothesis for this effect is the onset of behavioural changes in response to other epidemics in the US. An alternative explanation is that the estimates of the early growth rates of the epidemics in the states affected earliest are biased upwards by the early national ramp-up of surveillance and testing. Despite $R_{t=0}$ being highly variable, in part due to the factors discussed above, the majority of states have generally decreased their R_t since the first 10 deaths were observed (Figure 4). We estimate that 26 states have a posterior mean R_t of less than one but only 8 have 95% credible intervals that are completely below one. A posterior mean R_t below one and credible interval that includes one suggests that the epidemic is likely under control in that state, but the potential for increasing transmission cannot be ruled out. Therefore, our results show that very few states have conclusively controlled their epidemics. Of the ten states with the highest current R_t , half are in the Great Lakes region (Illinois, Ohio, Minnesota Indiana, and Wisconsin). In Figure 5 we show the geographical variation in the posterior probability that R_t is less than 1; green states are those with probability that R_t is below 1 is high, and pink states are those with low probability. The closer a value is to 100%, the more certain we are that the rate of transmission is below 1 and that new infections are not increasing at present. This is in contrast to many European countries that have conclusively reduced their R_t less than one at present [7].

¹We also considered the relationship of R_t with a population density weighted by proportion of the total population of the state in each census tract. This was less strongly correlated to $R_{t=0}$.

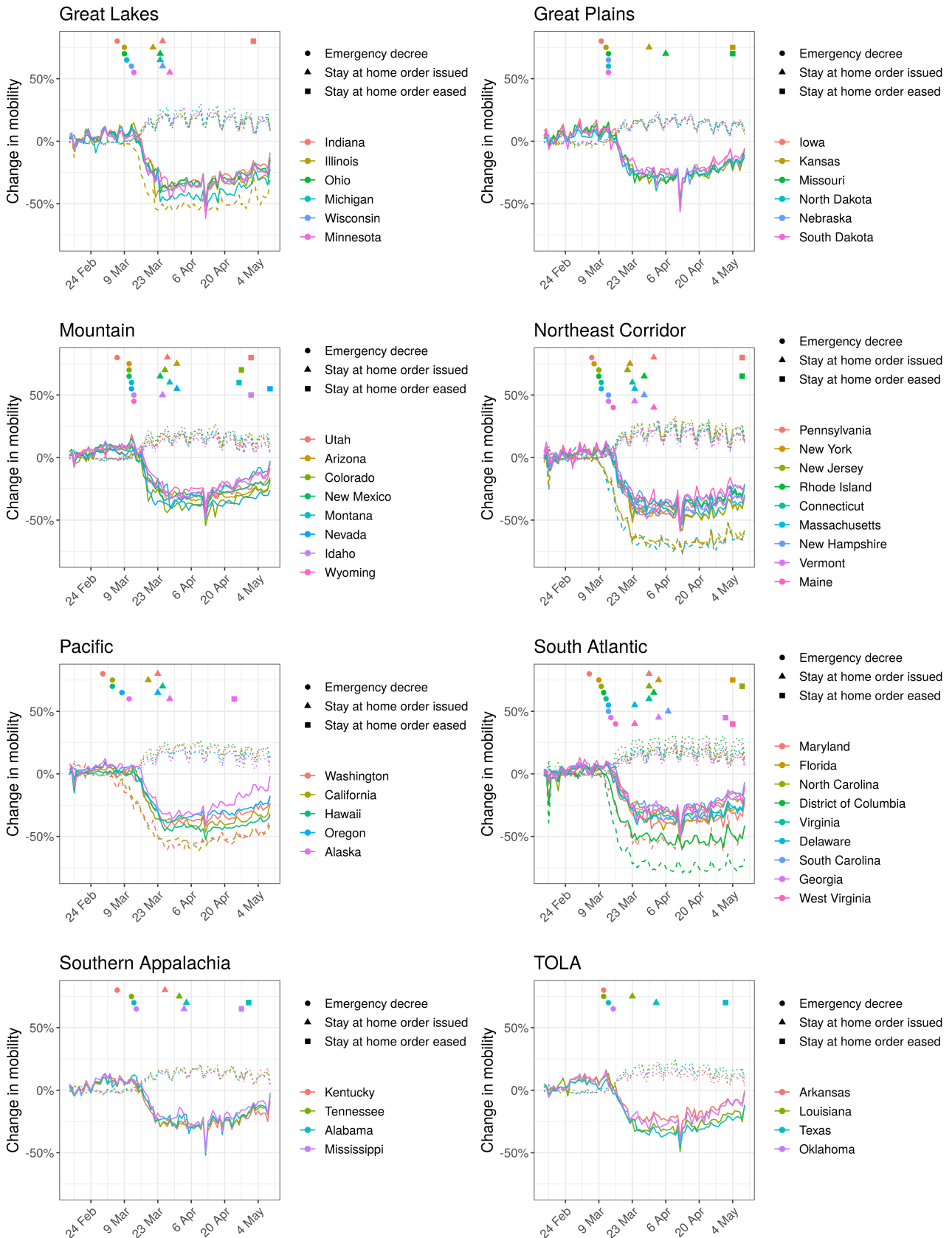


Figure 1: Comparison of mobility data from Google with government interventions for the 50 states and the District of Columbia. The solid lines show average mobility (across categories “retail & recreation”, “grocery & pharmacy”, “workplaces”), the dashed lines show “transit stations” and the dotted lines show “residential”. Intervention dates are indicated by shapes as shown in the legend; see Section 4 for more information about the interventions implemented. There is a strong correlation between the onset of interventions and reductions in mobility.

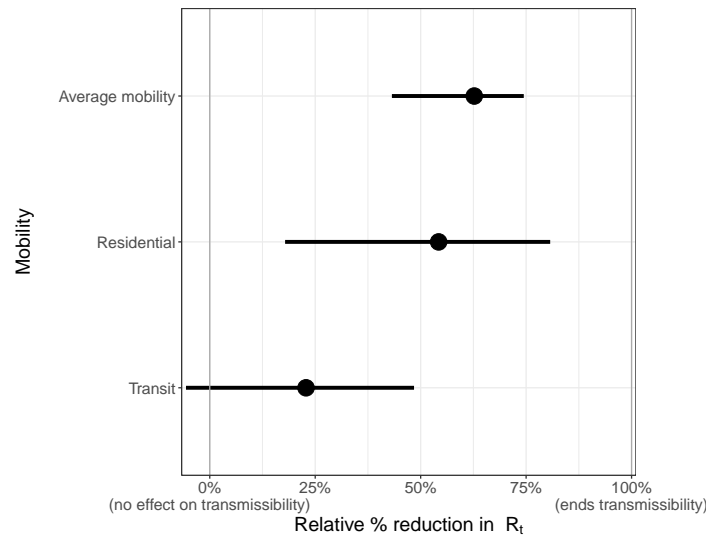


Figure 2: Covariate effect sizes: Average mobility combines “retail & recreation”, “grocery & pharmacy”, “workplaces”. Transit stations is only used as a covariate for states in which more than 20% of the working population commutes using public transportation. We plot estimates of the posterior mean effect sizes and 95% credible intervals for each mobility category. The relative % reduction in R_t metric is interpreted as follows: the larger the percentage, the more R_t decreases, meaning the disease spreads less; a 100% relative reduction ends disease transmissibility entirely. The smaller the percentage, the less effect the covariate has on transmissibility. A 0% relative reduction has no effect on R_t and thus no effect on the transmissibility of the disease, while a negative percent reduction implies an increase in transmissibility.

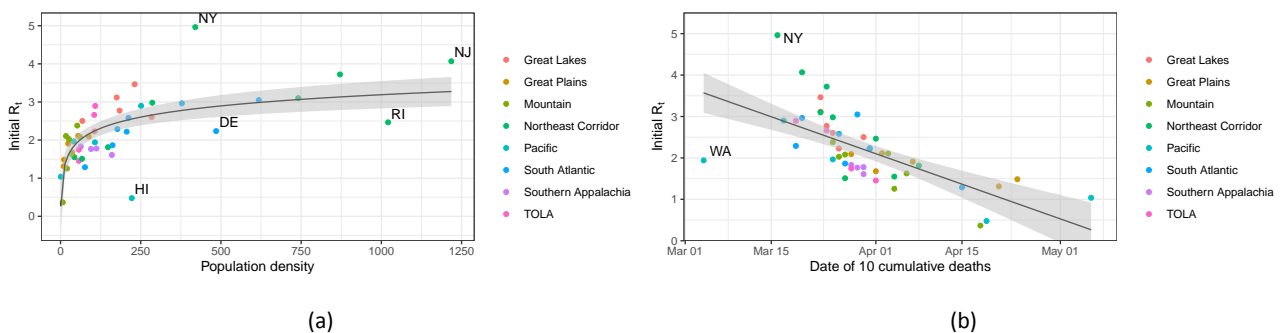


Figure 3: Comparison of initial $R_{t=0}$ with population density (a) and date of 10 cumulative deaths (b). R-squared values are 0.466 and 0.449 respectively.

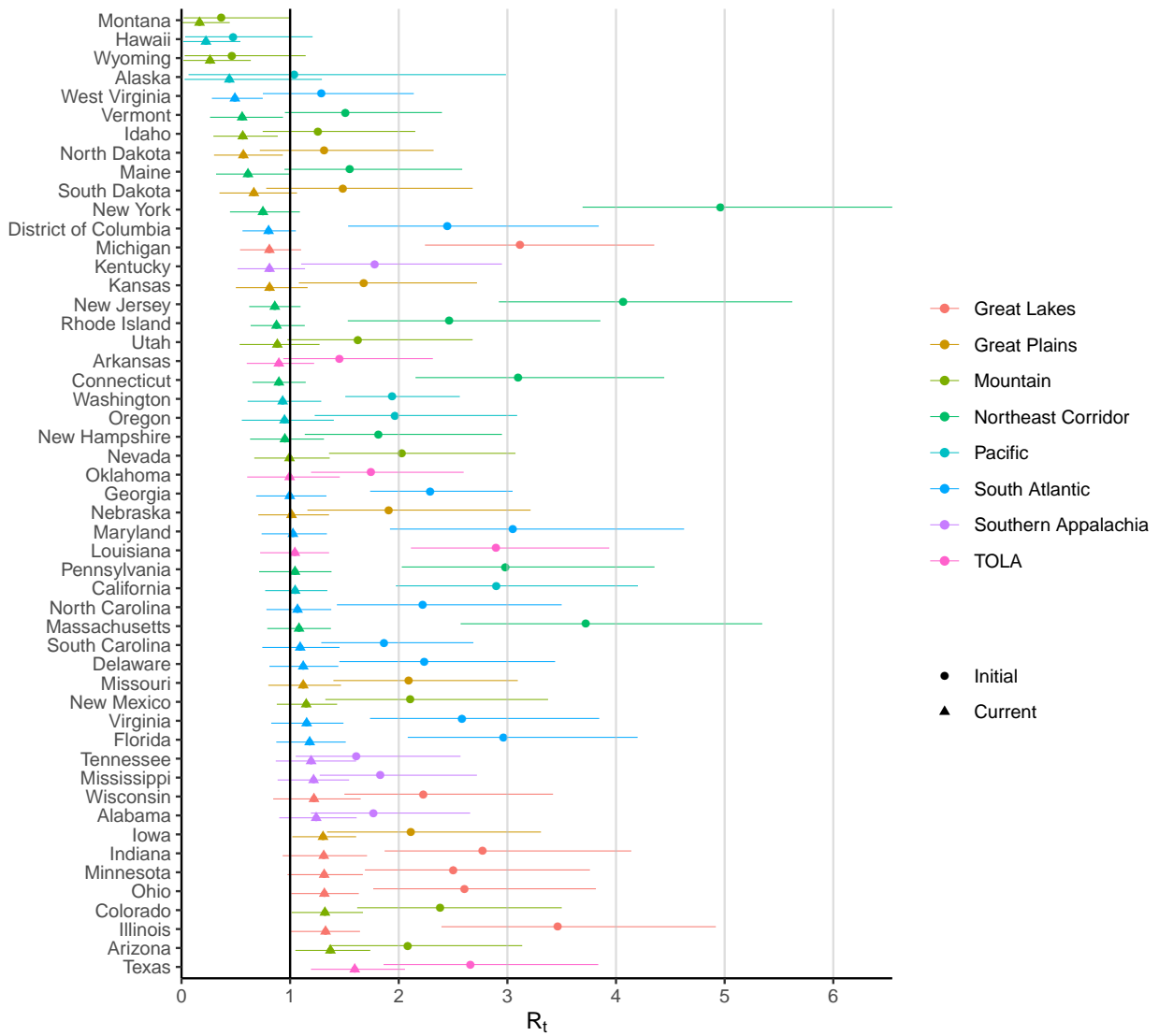


Figure 4: State-level estimates of initial R_t and the current average R_t over the past week. The colours indicate regional grouping as shown in Figure 1

Figure 5 shows that while we are confident that some states have controlled transmission, we are similarly confident that many states have not. Specifically, we are more than 50% sure that $R_t > 1$ in 25 states. There is substantial geographical clustering; most states in the Midwest and the South have rates of transmission that suggest the epidemic is not yet under control. We do note here that many states with $R_t < 1$ are still in the early epidemic phase with few deaths so far.

2.3 Trends in COVID-19 transmission

In this section we focus on five states: Washington, New York, Massachusetts, Florida, and California. These states represent a variety of COVID-19 government responses and outbreaks that have dominated the national discussion of

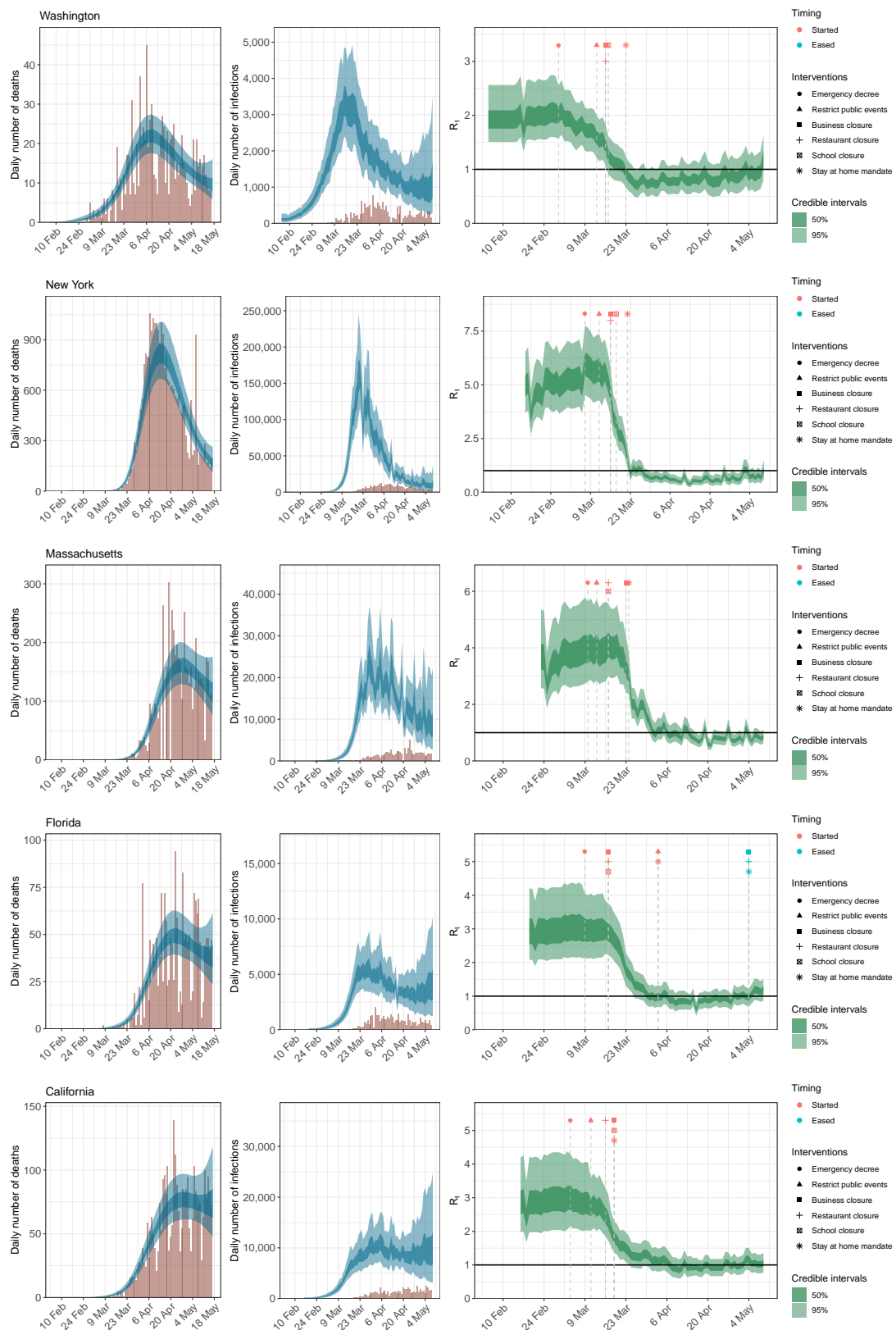


Figure 6: State-level estimates of infections, deaths, and R_t for Washington, New York, Massachusetts, Florida, and California. **Left:** daily number of deaths, brown bars are reported deaths, blue bands are predicted deaths, dark blue 50% credible interval (CI), light blue 95% CI. **Middle:** daily number of infections, brown bars are reported confirmed cases, blue bands are predicted infections, CIs are same as left. Afterwards, if the R_t is above 1, the number of infections will start growing again. **Right:** time-varying reproduction number R_t dark green 50% CI, light green 95% CI. Icons are interventions shown at the time they occurred.

Table 1: Posterior model estimates of percentage of total population infected as of 17 May 2020.

State	% of total population infected (mean [95% credible interval])	State	% of total population infected (mean [95% credible interval])
Alabama	1.9% [1.2%-3.0%]	Montana	0.2% [0.0%-0.4%]
Alaska	0.2% [0.0%-0.7%]	Nebraska	1.2% [0.7%-2.0%]
Arizona	2.3% [1.4%-4.0%]	Nevada	1.8% [1.3%-2.7%]
Arkansas	0.5% [0.3%-0.8%]	New Hampshire	2.2% [1.3%-3.6%]
California	1.6% [1.1%-2.5%]	New Jersey	16.1% [11.9%-21.7%]
Colorado	4.6% [3.1%-7.3%]	New Mexico	2.6% [1.6%-4.3%]
Connecticut	13.3% [9.7%-18.3%]	New York	16.6% [12.8%-21.6%]
Delaware	5.4% [3.5%-8.7%]	North Carolina	1.1% [0.7%-1.7%]
District of Columbia	10.8% [7.6%-15.4%]	North Dakota	0.9% [0.5%-1.6%]
Florida	1.3% [0.9%-2.0%]	Ohio	2.6% [1.7%-4.0%]
Georgia	2.7% [1.9%-3.8%]	Oklahoma	1.0% [0.7%-1.4%]
Hawaii	0.1% [0.0%-0.3%]	Oregon	0.4% [0.2%-0.6%]
Idaho	0.6% [0.3%-0.8%]	Pennsylvania	5.5% [3.7%-8.6%]
Illinois	7.1% [4.5%-11.2%]	Rhode Island	6.8% [4.8%-9.9%]
Indiana	5.0% [3.2%-7.9%]	South Carolina	1.2% [0.8%-1.8%]
Iowa	2.5% [1.5%-4.3%]	South Dakota	1.0% [0.5%-1.9%]
Kansas	0.9% [0.6%-1.3%]	Tennessee	0.7% [0.5%-1.2%]
Kentucky	1.0% [0.7%-1.4%]	Texas	1.4% [0.8%-2.4%]
Louisiana	8.0% [6.0%-11.0%]	Utah	0.5% [0.3%-0.9%]
Maine	0.5% [0.3%-0.8%]	Vermont	0.8% [0.5%-1.3%]
Maryland	5.6% [3.9%-8.3%]	Virginia	2.2% [1.4%-3.4%]
Massachusetts	13.0% [9.3%-18.3%]	Washington	1.9% [1.4%-2.7%]
Michigan	5.9% [4.5%-7.8%]	West Virginia	0.5% [0.3%-0.7%]
Minnesota	3.1% [1.8%-5.2%]	Wisconsin	1.2% [0.8%-1.8%]
Mississippi	3.8% [2.4%-6.1%]	Wyoming	0.3% [0.1%-0.6%]
Missouri	1.7% [1.1%-2.7%]	National	4.1% [3.7%-4.5%]

heterogeneity across states. New York and New Jersey have the highest estimated attack rates, of 16.6% [12.8%-21.6%] and 16.1% [11.9%-21.7%] respectively, and Connecticut, Massachusetts, and Washington, D.C. all have attack rates over 10%. Conversely, other states that have drawn attention for early outbreaks, such as California, Washington, and Florida, have attack rates of around 1%, and other states where the epidemic is still early, like Maine, having estimated attack rates of less than 1%. We note here that there is the possibility of under reporting of deaths in these states. Under reporting of COVID-19 attributable deaths will result in an underestimate of the attack rates. We note here that we have found our estimates to be reasonably robust in settings where there is significant under reporting (e.g. Brazil [9]).

Figure 7 shows the effective number of infectious individuals and the number of newly infected individuals on any given day for each of the 8 regions in our model. The effective number of infectious individuals is calculated using the generation time distribution, where individuals are weighted by how infectious they are over time. The fully infectious average includes asymptomatic and symptomatic individuals. Currently, we estimate that there are 1344000 [368000 - 3320000] infectious individuals across the whole of the US, which corresponds to 0.42% [0.11% - 1.03%] of the population. Table 2 shows the number currently infected across different states is highly heterogeneous. Figure 7 shows that despite new infections being in a steep decline, the number of people still infectious, and therefore able to sustain onward transmission, can still be large. This discrepancy underscores the importance of testing and case based isolation as a means to control transmission. We note that the expanding cone of uncertainty is in part due to uncertainties arising from the lag between infections and deaths, but also from trends in mobility. State level estimates of the total number of infectious individuals over time are given in Appendix E and the current number of infectious individuals are given in Figure 2.

2.5 Scenarios

The relationship between mobility and transmission is the principle mechanism affecting values of R_t in our model. Therefore, we illustrate the impact of likely near-term scenarios for R_t over the next 8 weeks, under assumptions of relaxations of interventions leading to increased mobility. We note that mobility is acting here as a proxy for the number of potentially infectious contacts. Our mobility scenarios [18] do not account for additional interventions that may be implemented, such as mass testing and contact tracing. It is also likely that when interventions are lifted behaviour may modify the effect sizes of mobility and reduce the impact of mobility on transmission. Factors such as increased use of masks and increased adherence to social distancing are examples. Given these factors we caution the reader to look at our scenarios as pessimistic, but illustrative of the potential risks.

We define scenarios based on percent return to baseline mobility, which is by definition 0. As an example, say that currently mobility is 50% lower than baseline, or -50%, perhaps due to the introduction of social-distancing NPIs. Then, a 20% increase of mobility from its current level is $-50\% * (1 - 20\%) = -40\%$. Similarly, if mobility in residences increased by 10% following a stay-at-home order, our 20% scenario reduces this to an 8% increase over baseline. This assumes that people have begun to resume pre-lockdown behaviour, but have not yet returned to baseline mobility. We hold this 20% return to baseline constant for the duration of the 8-week scenario.

We present three scenarios (a) constant mobility (mobility remains at current levels for 8 weeks), (b) 20% return to pre-stay-at-home mobility from current levels and (c) 40% return to pre-stay-at-home mobility from current levels. We justify

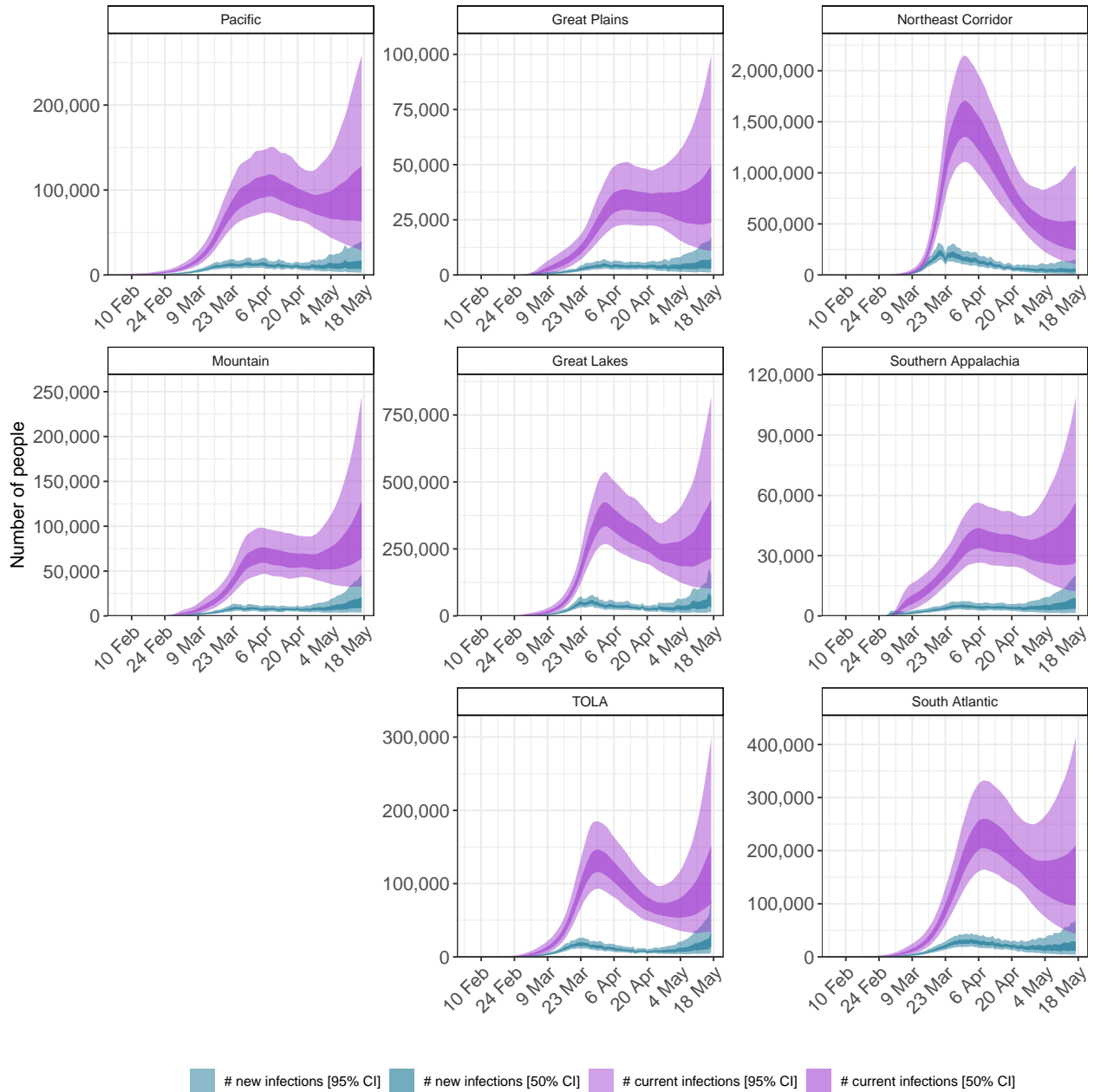


Figure 7: Estimates for the effective number of infectious individuals on a day in purple (light purple, 95% CI, dark purple 50% CI) and for newly infected people per day in blue (light blue, 95% CI, dark blue: 50% CI).

Table 2: Posterior model estimates of the number of currently infectious individuals as of 17 May 2020.

State	Number of infectious individuals (mean [95% credible interval])	State	Number of infectious individuals (mean [95% credible interval])
Alabama	15,000 [4,000-37,000]	Montana	0 [0-1,000]
Alaska	0 [0-2,000]	Nebraska	3,000 [0-10,000]
Arizona	40,000 [12,000-93,000]	Nevada	5,000 [0-14,000]
Arkansas	1,000 [0-4,000]	New Hampshire	4,000 [0-12,000]
California	92,000 [26,000-228,000]	New Jersey	94,000 [26,000-227,000]
Colorado	47,000 [15,000-110,000]	New Mexico	10,000 [2,000-24,000]
Connecticut	40,000 [11,000-93,000]	New York	84,000 [13,000-246,000]
Delaware	9,000 [2,000-22,000]	North Carolina	14,000 [3,000-35,000]
District of Columbia	7,000 [1,000-18,000]	North Dakota	0 [0-2,000]
Florida	39,000 [10,000-95,000]	Ohio	54,000 [17,000-125,000]
Georgia	28,000 [6,000-72,000]	Oklahoma	1,000 [0-5,000]
Hawaii	0 [0-1,000]	Oregon	1,000 [0-4,000]
Idaho	0 [0-1,000]	Pennsylvania	96,000 [23,000-251,000]
Illinois	176,000 [54,000-395,000]	Rhode Island	6,000 [1,000-16,000]
Indiana	52,000 [12,000-134,000]	South Carolina	7,000 [1,000-19,000]
Iowa	18,000 [5,000-41,000]	South Dakota	1,000 [0-5,000]
Kansas	1,000 [0-4,000]	Tennessee	6,000 [1,000-17,000]
Kentucky	2,000 [0-7,000]	Texas	90,000 [27,000-218,000]
Louisiana	29,000 [6,000-75,000]	Utah	1,000 [0-5,000]
Maine	0 [0-1,000]	Vermont	0 [0-1,000]
Maryland	37,000 [9,000-91,000]	Virginia	27,000 [6,000-66,000]
Massachusetts	96,000 [27,000-232,000]	Washington	9,000 [1,000-26,000]
Michigan	21,000 [4,000-59,000]	West Virginia	0 [0-1,000]
Minnesota	36,000 [10,000-88,000]	Wisconsin	7,000 [1,000-22,000]
Mississippi	22,000 [6,000-51,000]	Wyoming	0 [0-1,000]
Missouri	16,000 [4,000-41,000]	National	1344000 [368000 - 3320000]

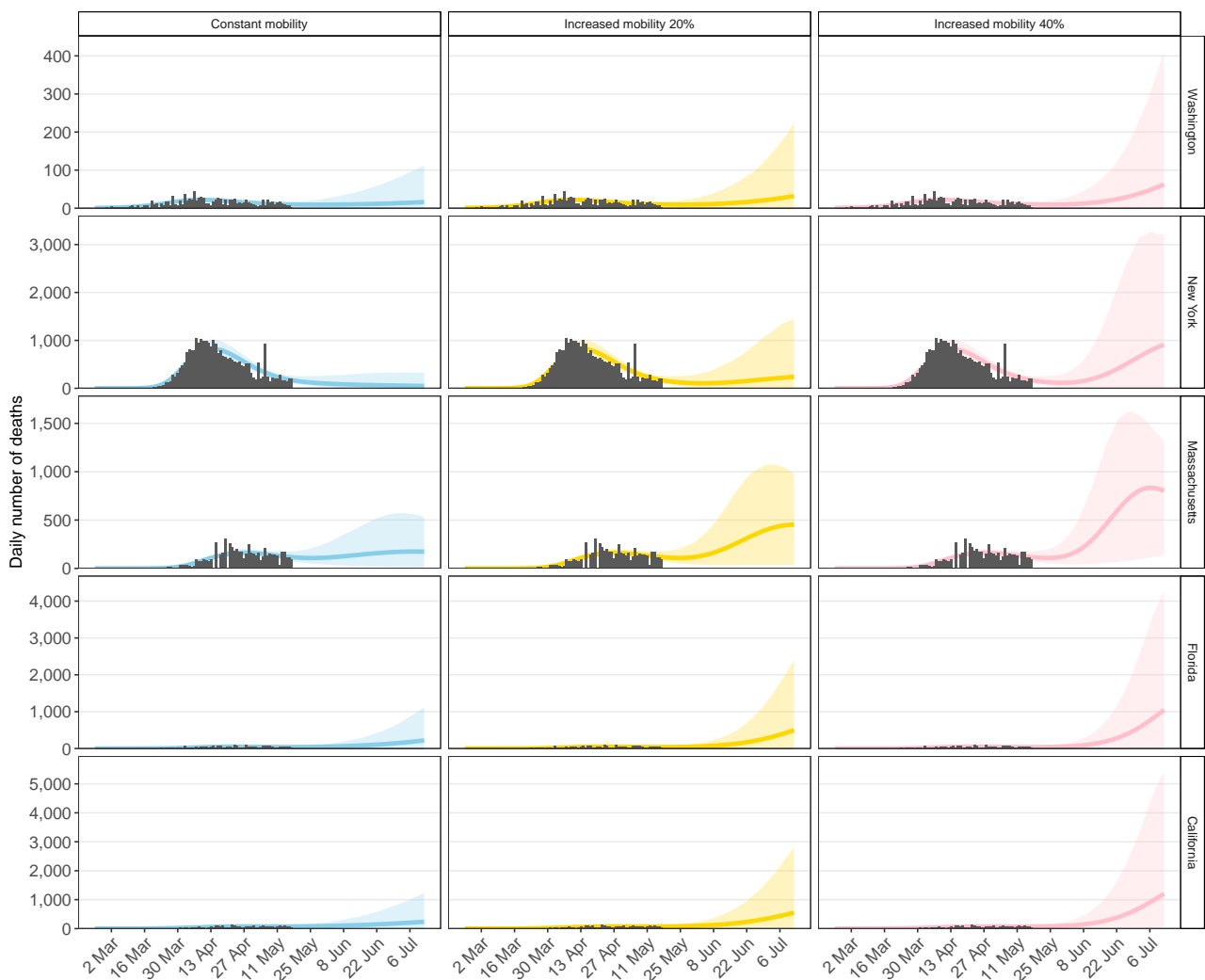


Figure 8: State-level scenario estimates of deaths for Washington, New York, Massachusetts, Florida and California. The ribbon shows the 95% credible intervals (CIs) for each scenario. The first column of plots show the results of scenario (a) where mobility is kept constant at pre-stay-at-home levels, the middle column shows results for scenario (b) where there is a 20% return to pre-epidemic mobility, and the right column shows scenario (c) where there is a 40% return to pre-epidemic mobility.

the selection of these scenarios by examining how mobility has changed in states that have already begun to relax social distancing guidelines. For example, Colorado's stay-at-home order expired on the 26th of April, and activity level reported by the Colorado Department of Public Health has recovered approximately 30% of the decrease observed following initial implementation of NPIs [6]. Figure 8 shows the estimated number of deaths for each scenario in the five states discussed above: Washington, New York, Massachusetts, Florida, and California. Results for all the states modelled are included in Appendix F. These estimates are certainly *not* forecasts and are based on multiple assumptions, but they illustrate the potential consequences of increasing mobility across the general population: in almost all cases, after 8 weeks, a 40% return to baseline leads to an epidemic larger than the current wave.

3 Conclusions

In this report we use a Bayesian semi-mechanistic model to investigate the impact of these NPIs via changes in mobility. Our model uses mobility to predict the rate of transmission, neglecting the potential effect of additional behavioural changes or interventions such as testing and tracing. While mobility will explain a large amount of the variance in R_t , there is likely to be substantial residual variation which will be geographically heterogeneous. We attempt to account for this residual variation through a second order, weekly, autoregressive process. This stochastic process is able to pick up variation driven by the data but is unable to determine associations or causal mechanisms. Figure 12 shows the residual variation captured by the autoregressive process, and given these lines are flat for the majority of states, we can conclude that much of the variation we see in the observed death data can be attributed to mobility. However, there are states, such as New York, where this residual effect is large which suggests that additional factors have contributed to the reduction in R_t . We hypothesise these could be behavioural changes but testing this hypothesis will require additional data.

We find that the starting reproduction number is associated with population density and the chronological date of epidemic onset. These two relationships suggest two dimensions which may influence the starting reproduction number and underscore the variability between states. We are cautious to draw any causal relationships from these associations; our results highlight that more additional studies of these factors are needed at finer spatial scales.

We find that the posterior mean of the current reproduction is above 1 in 9 states, with 95% confidence, and above 1 in 25 states with 50% confidence. These current reproduction numbers suggest that in many states the US epidemic is not under control and caution must be taken in loosening current interventions without additional measures in place. The high reproduction numbers are geographically clustered in the southern US and Great Plains region, while lower reproduction numbers are observed in areas that have suffered high COVID-19 mortality (such as the Northeast Corridor). We simulate forwards in time a partial return of mobility back to pre-COVID levels, while keeping all else constant, and find substantial resurgence is expected. In the majority of states, the deaths expected over a two-month period would exceed current levels by more than two-fold. This increase in mobility is modest and held constant for 8 weeks. However, these results must be heavily caveated: our results do not account for additional interventions that may be introduced such as mass testing, contact tracing and changing work place/transit practices. Our results also do not account for behavioural changes that may occur such as increased mask wearing or changes in age specific movement. Therefore, our scenarios are pessimistic in nature and should be interpreted as such. Given these caveats, we conjecture at the present time that, in the absence of additional interventions (such as mass testing), *additional* behavioural modifications are unlikely to substantially reduce R_t in of their own.

We estimate the number of individuals that have been infected by SARS-CoV2 to date. Our attack rates are sensitive to the assumed values of infection fatality rate (IFR). We account for each individual state's age structure, and further adjust for contact mixing patterns [19]. To ensure assumptions about IFR do not have undue influence on our conclusions, we incorporate prior noise in the estimate, and perform a sensitivity analysis using different contact matrices. Also, our attack rates for New York are in line with those from recent serological studies [1]. We show that while reductions in the daily infections continue, the reservoir of infectious individuals remains large. This reservoir also implies that interventions should remain in place longer than the daily case count implies, as trends in the number of infectious individuals lags behind. The magnitude of difference between newly infected and currently infected individuals suggest that mass testing

and isolation could be an effective intervention.

Our results suggest that while the US has substantially reduced its reproduction numbers in all states, there is little evidence that the epidemic is under control in the majority of states. Without changes in behaviour that result in reduced transmission, or interventions such as increased testing that limit transmission, new infections of COVID-19 are likely to persist, and, in the majority of states, grow.

4 Data

Our model uses daily real-time state-level aggregated data published by New York Times (NYT) [20] for New York State and John Hopkins University (JHU) [3] for the remaining states. There is no single source of consistent and reliable data for all 50 states. We acknowledge that data issues such as under reporting and time lags can influence our results. In previous reports [8, 9, 7] we have shown our modelling methodology is generally robust to these data issues due to pooling. However, we do recognise no modelling methodology will be able to surmount all data issues; therefore these results should be interpreted as the best estimates based on current data, and are subject to change with future data consolidation. JHU and NYT provide information on confirmed cases and deaths attributable to COVID-19, however again, the case data are highly unrepresentative of the incidence of infections due to under-reporting and systematic and state-specific changes in testing. We, therefore, use only deaths attributable to COVID-19 in our model. While the observed deaths still have some degree of unreliability, again due to changes in reporting and testing, we believe the data are of sufficient fidelity to model. For age specific population counts we use data from the U.S. Census Bureau in 2018 [21]. The timing of social distancing measures was collated by the University of Washington [11].

We use the Google Mobility Report [5]³ which provides data on movement in the USA by states and highlights the percent change in visits to:

- Grocery & pharmacy: Mobility trends for places like grocery markets, food warehouses, farmers markets, speciality food shops, drug stores, and pharmacies.
- Parks: Mobility trends for places like local parks, national parks, public beaches, marinas, dog parks, plazas, and public gardens.
- Transit stations: Mobility trends for places like public transport hubs such as subway, bus, and train stations.
- Retail & recreation: Mobility trends for places like restaurants, cafes, shopping centres, theme parks, museums, libraries, and movie theatres.
- Residential: Mobility trends for places of residence.
- Workplaces: Mobility trends for places of work.

The mobility data show length of stay at different places compared to a baseline. It is therefore relative, i.e. mobility of -20% means that, compared to normal circumstances individuals are engaging in a given activity 20% less.

³We use mobility data from Google, which was last updated on 9th May 2020. For dates after 9th May 2020, we impute the mobility data with the median of last seven days.

5 Methods

We introduced a new Bayesian framework for estimating the transmission intensity and attack rate (percentage of the population that has been infected) of COVID-19 from the reported number of deaths in a previous report [7]⁴. This framework uses the time-varying reproduction number R_t to inform a latent function for infections, and then these infections, together with probabilistic lags, are calibrated against observed deaths. Observed deaths, while still susceptible to under reporting and delays, are more reliable than the reported number of confirmed cases, although the early focus of most surveillance systems on cases with reported travel histories to China may have missed some early deaths. Changes in testing strategies during the epidemic mean that the severity of confirmed cases as well as the reporting probabilities changed in time and may thus have introduced bias in the data.

In this report, we adapt our original Bayesian semi-mechanistic model of the infection cycle to the states in the USA. We infer plausible upper and lower bounds (Bayesian credible intervals) of the total populations infected (attack rates) and the reproduction number over time (R_t). In our framework we parametrize R_t as a function of Google mobility data. We fit the model jointly to COVID-19 data from all regions to assess whether there is evidence that changes in mobility have so far been successful at reducing R_t below 1. Our model is a partial pooling model, where the effect of mobility is shared, but region- and state-specific modifiers can capture differences and idiosyncrasies among the regions.

We note that future directions should focus on embedding mobility in realistic contact mechanisms to establish a closer relationship to transmission.

5.1 Model specifics

We observe daily deaths $D_{t,m}$ for days $t \in \{1, \dots, n\}$ and states $m \in \{1, \dots, M\}$. These daily deaths are modelled using a positive real-valued function $d_{t,m} = \mathbb{E}[D_{t,m}]$ that represents the expected number of deaths attributed to COVID-19. The daily deaths $D_{t,m}$ are assumed to follow a negative binomial distribution with mean $d_{t,m}$ and variance $d_{t,m} + \frac{d_{t,m}^2}{\psi}$, where ψ follows a positive half normal distribution, i.e.

$$D_{t,m} \sim \text{Negative Binomial} \left(d_{t,m}, d_{t,m} + \frac{d_{t,m}^2}{\psi} \right),$$

$$\psi \sim \mathcal{N}^+(0, 5).$$

Here, $\mathcal{N}(\mu, \sigma)$ denotes a normal distribution with mean μ and standard deviation σ . We say that X follows a positive half normal distribution $\mathcal{N}^+(0, \sigma)$ if $X \sim |Y|$, where $Y \sim \mathcal{N}(0, \sigma)$.

To mechanistically link our function for deaths to our latent function for infected cases, we use a previously estimated COVID-19 infection fatality ratio (IFR, probability of death given infection) together with a distribution of times from infection to death π . Details of this calculation can be found in [22, 23]. From the above, every region has a specific mean infection fatality ratio ifr_m (see Appendix G). To incorporate the uncertainty inherent in this estimate we allow the

⁴Similar to our previous report [7], we seed each epidemic for 5 consecutive days starting 30 days before the state reached ten cumulative deaths. Wyoming did not report more than 10 deaths in our data set, so we use a threshold of five instead.

ifr_m for every state to have additional noise around the mean. Specifically we assume

$$\text{ifr}_m^* \sim \text{ifr}_m \cdot \mathcal{N}(1, 0.1).$$

We believe a large-scale contact survey similar to polymod [19] has not been collated for the USA, so we assume the contact patterns are similar to those in the UK. We conducted a sensitivity analysis, shown in Appendix G, and found that the IFR calculated using the contact matrices of other European countries lay within the posterior of ifr_m^* .

Using estimated epidemiological information from previous studies [22, 23], we assume the distribution of times from infection to death π (infection-to-death) to be

$$\pi \sim \text{Gamma}(5.1, 0.86) + \text{Gamma}(17.8, 0.45).$$

The expected number of deaths $d_{t,m}$, on a given day t , for state m is given by the following discrete sum:

$$d_{t,m} = \text{ifr}_m^* \sum_{\tau=0}^{t-1} c_{\tau,m} \pi_{t-\tau},$$

where $c_{\tau,m}$ is the number of new infections on day τ in state m and where π is discretized via $\pi_s = \int_{s-0.5}^{s+0.5} \pi(\tau) d\tau$ for $s = 2, 3, \dots$, and $\pi_1 = \int_0^{1.5} \pi(\tau) d\tau$, where $\pi(\tau)$ is the density of π .

The true number of infected individuals, c , is modelled using a discrete renewal process. We specify a generation distribution g with density $g(\tau)$ as:

$$g \sim \text{Gamma}(6.5, 0.62).$$

Given the generation distribution, the number of infections $c_{t,m}$ on a given day t , and state m , is given by the following discrete convolution function:

$$c_{t,m} = S_{t,m} R_{t,m} \sum_{\tau=0}^{t-1} c_{\tau,m} g_{t-\tau}, \quad (1)$$

$$S_{t,m} = 1 - \frac{\sum_{i=0}^{t-1} c_{i,m}}{N_m}$$

where, similar to the probability of death function, the generation distribution is discretized by $g_s = \int_{s-0.5}^{s+0.5} g(\tau) d\tau$ for $s = 2, 3, \dots$, and $g_1 = \int_0^{1.5} g(\tau) d\tau$. The population of state m is denoted by N_m . We include the adjustment factor $S_{t,m}$ to account for the number of susceptible individuals left in the population.

We parametrise $R_{t,m}$ as a linear function of the relative change in time spent (from a baseline)

$$R_{t,m} = R_{0,m} \cdot f\left(-\left(\sum_{k=1}^3 X_{t,m,k} \alpha_k\right) - Y_{t,m} \alpha_{r(m)}^{\text{region}} - Z_{t,m} \alpha_m^{\text{state}} - \epsilon_{m,w_m(t)}\right), \quad (2)$$

where $f(x) = 2 \exp(x)/(1 + \exp(x))$ is twice the inverse logit function. $X_{t,m,k}$ are covariates that have the same effect for all states, $Y_{t,m}$ is a covariate that also has a region-specific effect, $r(m) \in \{1, \dots, R\}$ is the region a state is in (see Figure 1), $Z_{t,m}$ is a covariate that has a state-specific effect and $\epsilon_{m,w_m(t)}$ is a weekly AR(2) process, centred around 0, that captures variation between states that is not explained by the covariates.

The prior distribution for $R_{0,m}$ [24] was chosen to be

$$R_{0,m} \sim \mathcal{N}(3.28, \kappa) \text{ with } \kappa \sim \mathcal{N}^+(0, 0.5),$$

where κ is the same among all states.

In the analysis of this paper we chose the following covariates: $X_{t,m,1} = M_{t,m}^{\text{average}}$, $X_{t,m,2} = M_{t,m}^{\text{transit}}$, $X_{t,m,3} = M_{t,m}^{\text{residential}}$, $Y_{t,m} = M_{t,m}^{\text{average}}$, and $Z_{t,m} = M_{t,m}^{\text{transit}}$, where the mobility variables are from [5] and defined as follows (all are encoded so that 0 is the baseline and 1 is a full reduction of the mobility in this dimension):

- $M_{t,m}^{\text{average}}$ is an average of retail and recreation, groceries and pharmacies, and workplaces. An average is taken as these dimensions are strongly collinear.
- $M_{t,m}^{\text{transit}}$ is encoding mobility for public transport hubs. For states where less than 20% of the working population aged 16 and over uses public transportation, we set $M_{t,m}^{\text{transit}} = 0$, i.e. this mobility has no effect on transmission. For states in which more than 20% of the working population commutes using public transportation, $M_{t,m}^{\text{transit}}$ is the mobility on transit.
- $M_{t,m}^{\text{residential}}$ are the mobility trends for places of residences.

The weekly, state-specific effect is modelled as a weekly AR(2) process, centred around 0 with stationary standard deviation σ_w that starts on the day after the emergency decree in a state. Before the emergency decree, there is no random weekly effect, so $\epsilon_{1,m} = 0$. Afterwards, the AR(2) process starts with $\epsilon_{2,m} \sim \mathcal{N}(0, \sigma_w^*)$,

$$\epsilon_{w,m} \sim \mathcal{N}(\rho_1 \epsilon_{w-1,m} + \rho_2 \epsilon_{w-2,m}, \sigma_w^*) \text{ for } m = 3, 4, \dots \quad (3)$$

with independent priors on ρ_1 and ρ_2 that are normal distributions conditioned to be in $[0, 1]$; the prior for ρ_1 is a $\mathcal{N}(0.8, .05)$ distribution conditioned to be in $[0, 1]$ the prior for ρ_2 is a $\mathcal{N}(0.1, .05)$ distribution, conditioned to be in $[0, 1]$. The prior for σ_w , the standard deviation of the stationary distribution of ϵ_w is chosen as $\sigma_w \sim \mathcal{N}^+(0, .2)$. The standard deviation of the weekly updates to achieve this standard deviation of the stationary distribution is $\sigma_w^* = \sigma_w \sqrt{1 - \rho_1^2 - \rho_2^2 - 2\rho_1\rho_2/(1 - \rho_2)}$.

The conversion from days to weeks is encoded in $w_m(t)$. We set $w_m(t) = 1$ for all $t \leq t_m^{\text{emergency}}$, which is the day of the emergency decree in that state. Then, every 7 days, w_m is incremented, i.e. $w_m(t) = \lfloor \max(t - t_m^{\text{emergency}} - 1, 0) / 7 \rfloor + 2$ for $t > t_m^{\text{emergency}}$. Due to the lag between infection and death, our estimates of R_t in the last two weeks before the end of our observations are (almost) not informed by corresponding death data. Therefore, we assume that the last two weeks have the same random weekly effect as the week 3 weeks before the end of observation.

The prior distribution for the shared coefficients were chosen to be

$$\alpha_k \sim \mathcal{N}(0, 0.5), k = 1, \dots, 3,$$

and the prior distribution for the pooled coefficients were chosen to be

$$\alpha_r^{\text{region}} \sim \mathcal{N}(0, \gamma_r), r = 1, \dots, R, \text{ with } \gamma_r \sim \mathcal{N}^+(0, 0.5),$$

$$\alpha_m^{\text{state}} \sim \mathcal{N}(0, \gamma_s), m = 1, \dots, M \text{ with } \gamma_s \sim \mathcal{N}^+(0, 0.5).$$

We assume that seeding of new infections begins 30 days before the day after a state has cumulatively observed 10 deaths. From this date, we seed our model with 6 sequential days of an equal number of infections: $c_{1,m} = \dots =$

$c_{6,m} \sim \text{Exponential}(\frac{1}{\tau})$, where $\tau \sim \text{Exponential}(0.03)$. These seed infections are inferred in our Bayesian posterior distribution.

We estimated parameters jointly for all states in a single hierarchical model. Fitting was done in the probabilistic programming language Stan[25] using an adaptive Hamiltonian Monte Carlo (HMC) sampler.

6 Acknowledgements

We would like to thank Amazon AWS and Microsoft Azure for computational credits and we would like to thank the Stan development team for their ongoing assistance. This work was supported by Centre funding from the UK Medical Research Council under a concordat with the UK Department for International Development, the NIHR Health Protection Research Unit in Modelling Methodology and Community Jameel.

References

- [1] S M Kissler et al. "Reductions in commuting mobility predict geographic differences in SARS-CoV-2 prevalence in New York City". In: (2020). URL: <http://nrs.harvard.edu/urn-3:HUL.InstRepos:42665370>.
- [2] Santa Clara County Public Health. *County of Santa Clara Identifies Three Additional Early COVID-19 Deaths*. 2020. URL: <https://www.sccgov.org/sites/covid19/Pages/press-release-04-21-20-early.aspx>.
- [3] E Dong, H Du, and L Gardner. "An interactive web-based dashboard to track COVID-19 in real time". eng. In: *The Lancet. Infectious diseases* (Feb. 2020), pp. 1473–3099. ISSN: 1474-4457. URL: <https://pubmed.ncbi.nlm.nih.gov/32087114https://www.ncbi.nlm.nih.gov/pmc/articles/PMC7159018/>.
- [4] C Courtemanche et al. "Strong Social Distancing Measures In The United States Reduced The COVID-19 Growth Rate". In: *Health Affairs* 39.7 (2020).
- [5] A Aktay et al. "Google COVID-19 Community Mobility Reports: Anonymization Process Description (version 1.0)". In: *ArXiv abs/2004.0* (2020).
- [6] J Bayham et al. *Colorado Mobility Patterns During the COVID-19 Response*. 2020. URL: http://www.ucdenver.edu/academics/colleges/PublicHealth/coronavirus/Documents/Mobility%20Report_final.pdf.
- [7] S Flaxman et al. *Report 13: Estimating the number of infections and the impact of non-pharmaceutical interventions on COVID-19 in 11 European countries*. 2020.
- [8] M Vollmer et al. *Report 20: Using mobility to estimate the transmission intensity of COVID-19 in Italy: A subnational analysis with future scenarios*. 2020.
- [9] T A Mellan et al. *Report 21 - Estimating COVID-19 cases and reproduction number in Brazil*. 2020.
- [10] M. Reston, K. Sgueglia, and C. Mossburg. *Governors on East and West coasts form pacts to decide when to reopen economies*. 2020. URL: <https://edition.cnn.com/2020/04/13/politics/states-band-together-reopening-plans/index.html>.

- [11] N Fullman et al. *State-level social distancing policies in response to COVID-19 in the US*. 2020. URL: <http://www.covid19statepolicy.org>.
- [12] United States Census Bureau. *Explore Census Data*. 2020. URL: <https://data.census.gov/cedsci/>.
- [13] Morning Consult. *How the Coronavirus Outbreak Is Impacting Public Opinion*. Accessed on 15/05/2020. 2020. URL: <https://morningconsult.com/form/coronavirus-outbreak-tracker/>.
- [14] J Stromberg. *The real reason American public transportation is such a disaster*. 2015. URL: <https://www.vox.com/2015/8/10/9118199/public-transportation-subway-buses>.
- [15] B D Dalziel et al. "Urbanization and humidity shape the intensity of influenza epidemics in U.S. cities". In: *Science* 362.6410 (2018), pp. 75–79. ISSN: 0036-8075. eprint: <https://science.sciencemag.org/content/362/6410/75.full.pdf>. URL: <https://science.sciencemag.org/content/362/6410/75>.
- [16] City and County of Department of Public Health San Francisco. *ORDER OF THE HEALTH OFFICER No. C19-07c*. 2020. URL: <https://sf.gov/sites/default/files/2020-04/2020.04.29%20FINAL%20%28signed%29%20Health%20Officer%20Order%20C19-07c-%20Shelter%20in%20Place.pdf>.
- [17] L Gamio S Mervosh J Lee and N Popovich. *See Which States Are Reopening and Which Are Still Shut Down*. 2020. URL: <https://www.nytimes.com/interactive/2020/us/states-reopen-map-coronavirus.html>.
- [18] KEC Ainslie et al. "Evidence of initial success for China exiting COVID-19 social distancing policy after achieving containment". In: *Wellcome Open Research* 5.81 (2020).
- [19] J Mossong et al. "Social Contacts and Mixing Patterns Relevant to the Spread of Infectious Diseases". In: *PLOS Medicine* 5.3 (Mar. 2008), pp. 1–1. URL: <https://doi.org/10.1371/journal.pmed.0050074>.
- [20] M Smith et al. *Coronavirus (Covid-19) Data in the United States*. 2020. URL: <https://github.com/nytimes/covid-19-data>.
- [21] Census reporter. *Census reporter*. 2020. URL: <https://censusreporter.org>.
- [22] R Verity et al. "Estimates of the severity of COVID-19 disease". In: *Lancet Infect Dis* (2020).
- [23] P Walker et al. *Report 12: The Global Impact of COVID-19 and Strategies for Mitigation and Suppression*. 2020. URL: <https://www.imperial.ac.uk/mrc-global-infectious-disease-analysis/news--wuhan-coronavirus/>.
- [24] Y Liu et al. "The reproductive number of COVID-19 is higher compared to SARS coronavirus". In: *Journal of Travel Medicine* (2020). ISSN: 17088305.
- [25] B Carpenter et al. "Stan: A Probabilistic Programming Language". In: *Journal of Statistical Software* 76.1 (2017), pp. 1–32. ISSN: 1548-7660. URL: <http://www.jstatsoft.org/v76/i01/>.

A Mobility regression analysis

In Figure 9 we regress NPIs against average mobility. We parameterise NPIs as piece-wise constant functions that are zero when the intervention has not been implemented and one when it has. We evaluate the correlation between the predictions from the linear model and the actual average mobility. We also lag the timing of interventions and investigate its impact on predicted correlation.

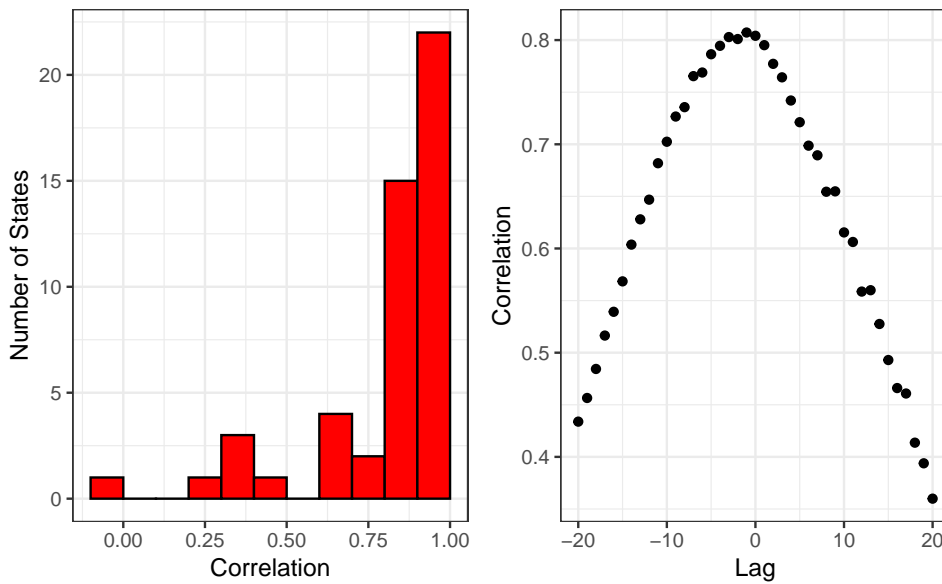


Figure 9: Mobility regression analysis.

B Effect sizes

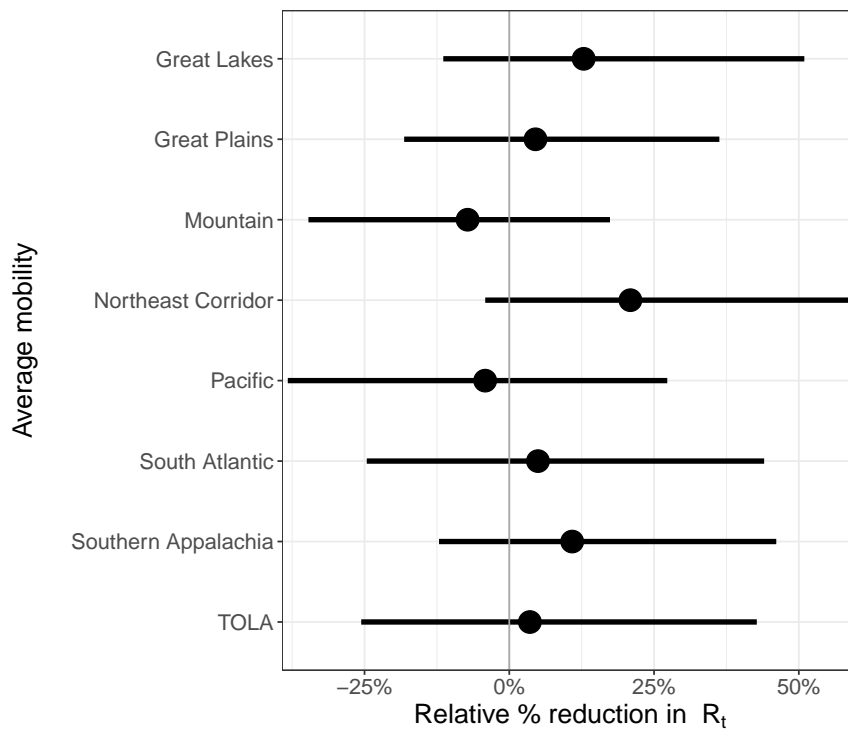


Figure 10: Regional covariate effect size plots.

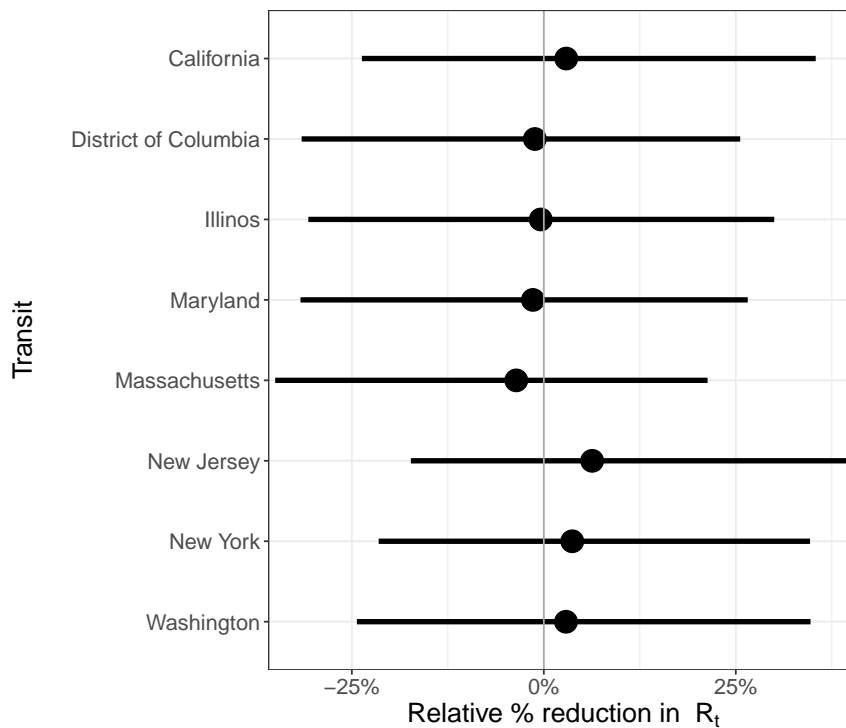


Figure 11: State-level covariate effect size plots.

C State-specific weekly effects after emergency decree

Our model includes a state-specific weekly effect $\epsilon_{w,m}$ (see equations 2, 3) for every week w after the emergency decree of that state. As described in Section 5, We assign an autoregressive process with mean 0 as prior to this effect. This weekly effect is held constant for the 4 weeks up to the present week. Figure 12 shows the posterior of this effect on the same scale as in Figure 2, that is, the percent reduction in R_t with mobility variables held constant⁵. Values above 0 have the interpretation that the state-specific weekly effect lowers the reproduction number $R_{t,m}$, i.e. transmission for week t and state m is lower than what is explained by the mobility covariates.

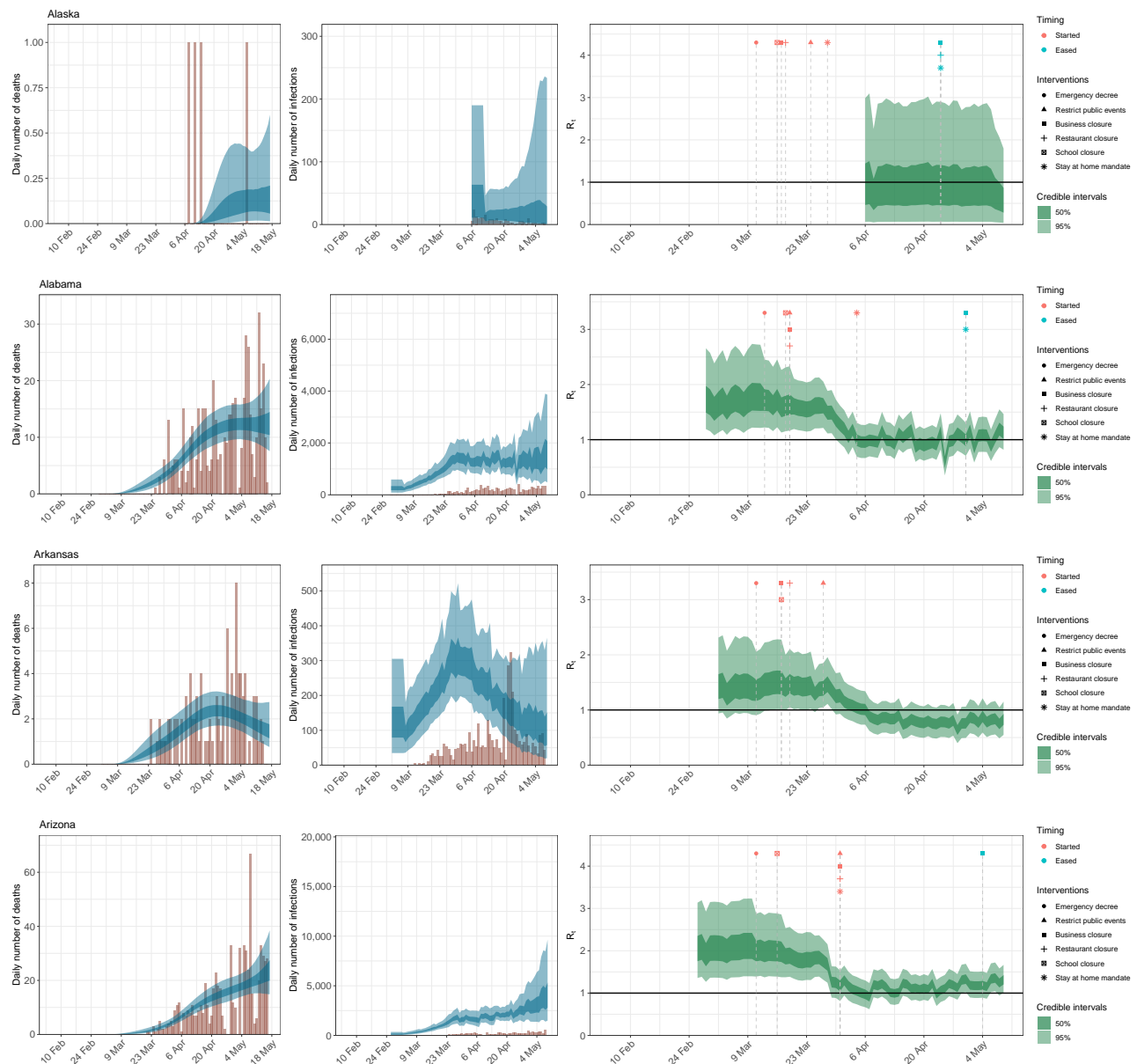
⁵Draws from the posterior are transformed with $1 - f(-\epsilon_{m,w_m(t)})$, where $f(x) = 2 \exp(x)/(1 + \exp(x))$ is twice the inverse logit function.

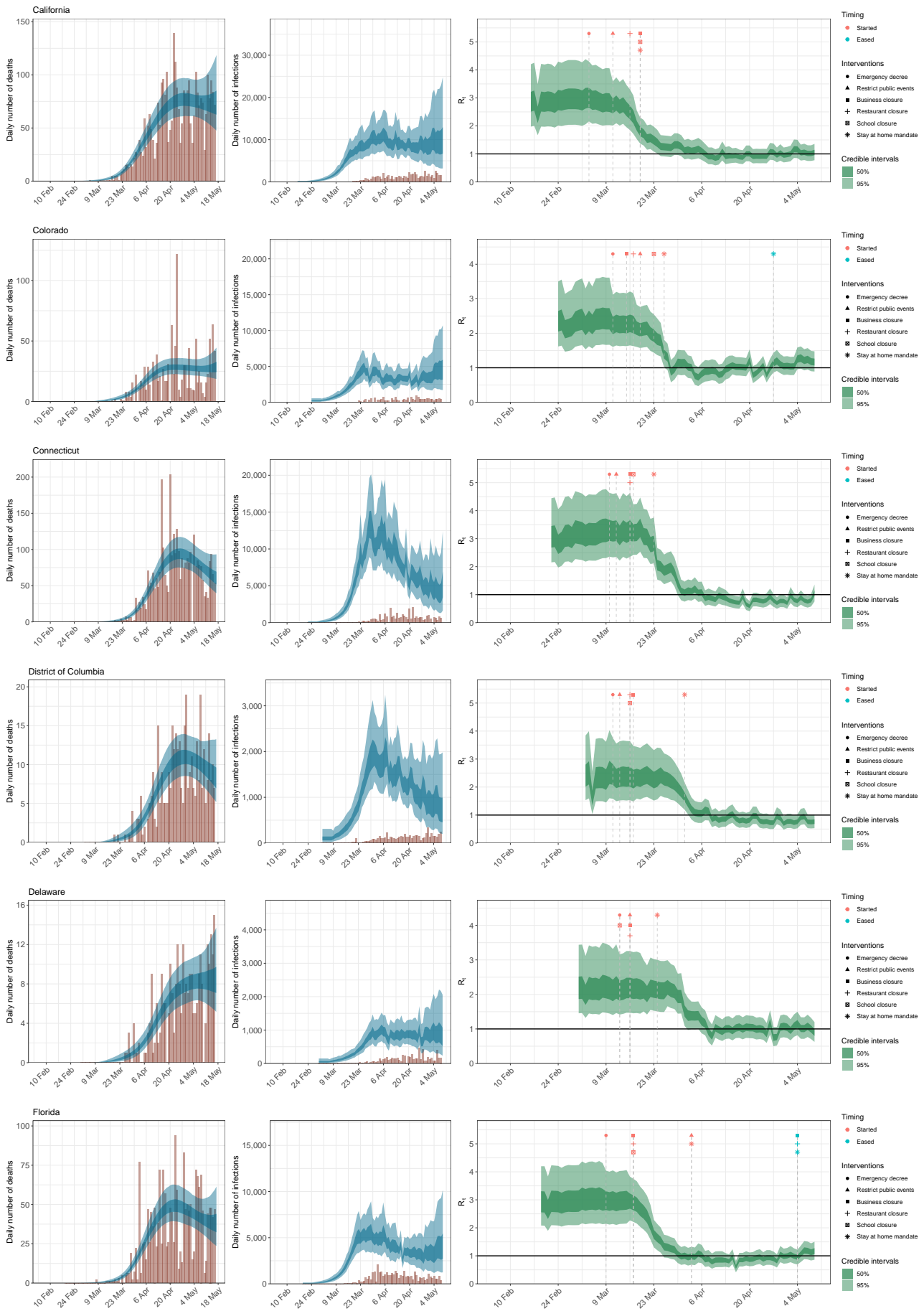


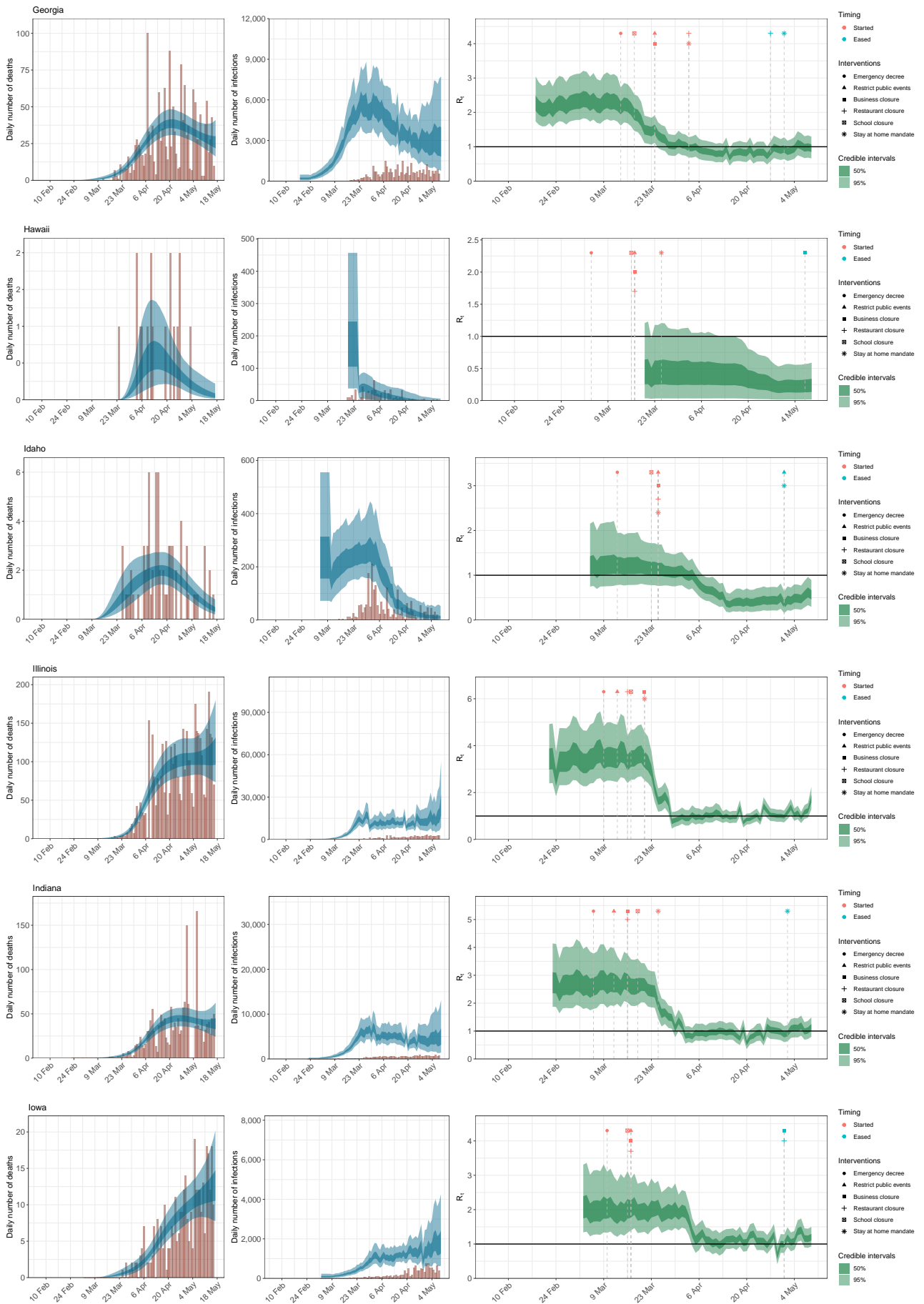
Figure 12: Percent reduction in R_t due to the weekly, state-level autoregressive effect after the emergency decree.

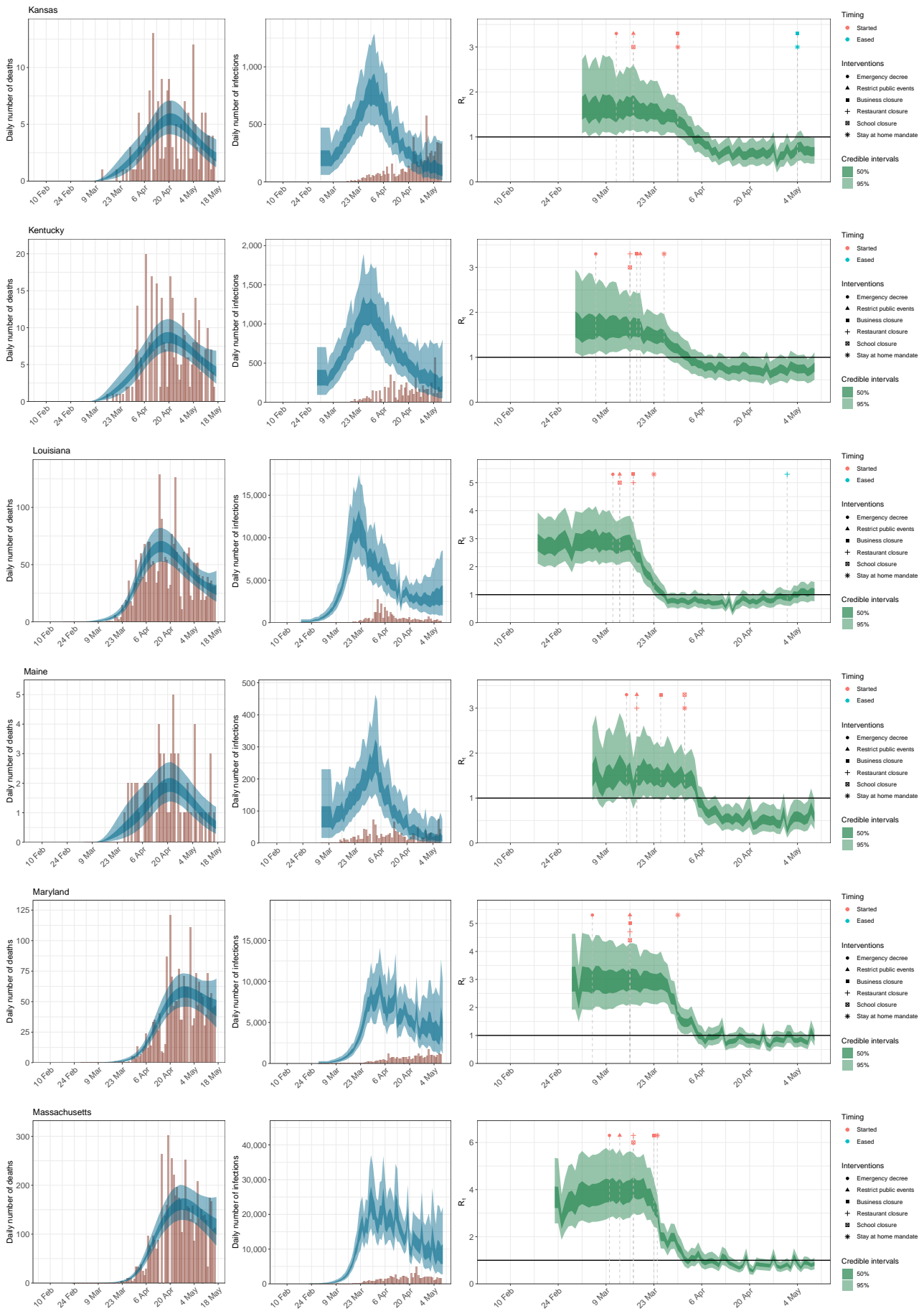
D Model predictions for all states

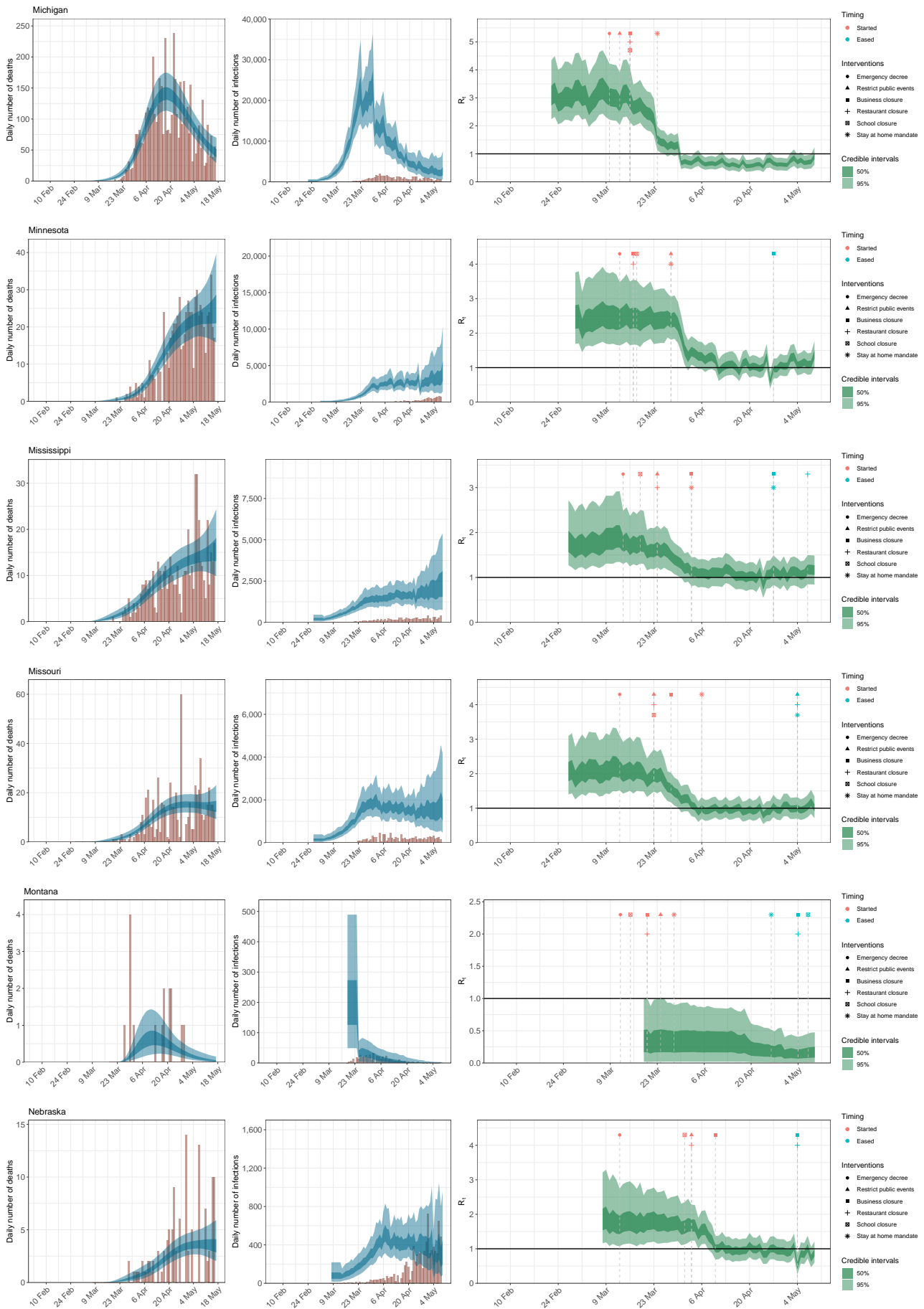
State-level estimates of infections, deaths and R_t . Left: daily number of deaths, brown bars are reported deaths, blue bands are predicted deaths, dark blue 50% credible interval (CI), light blue 95% CI. Middle: daily number of infections, brown bars are reported infections, blue bands are predicted infections, CIs are same as left. The number of daily infections estimated by our model drops immediately after an intervention, as we assume that all infected people become immediately less infectious through the intervention. Afterwards, if the R_t is above 1, the number of infections will start growing again. Right: time-varying reproduction number R_t dark green 50% CI, light green 95% CI. Icons are interventions shown at the time they occurred.

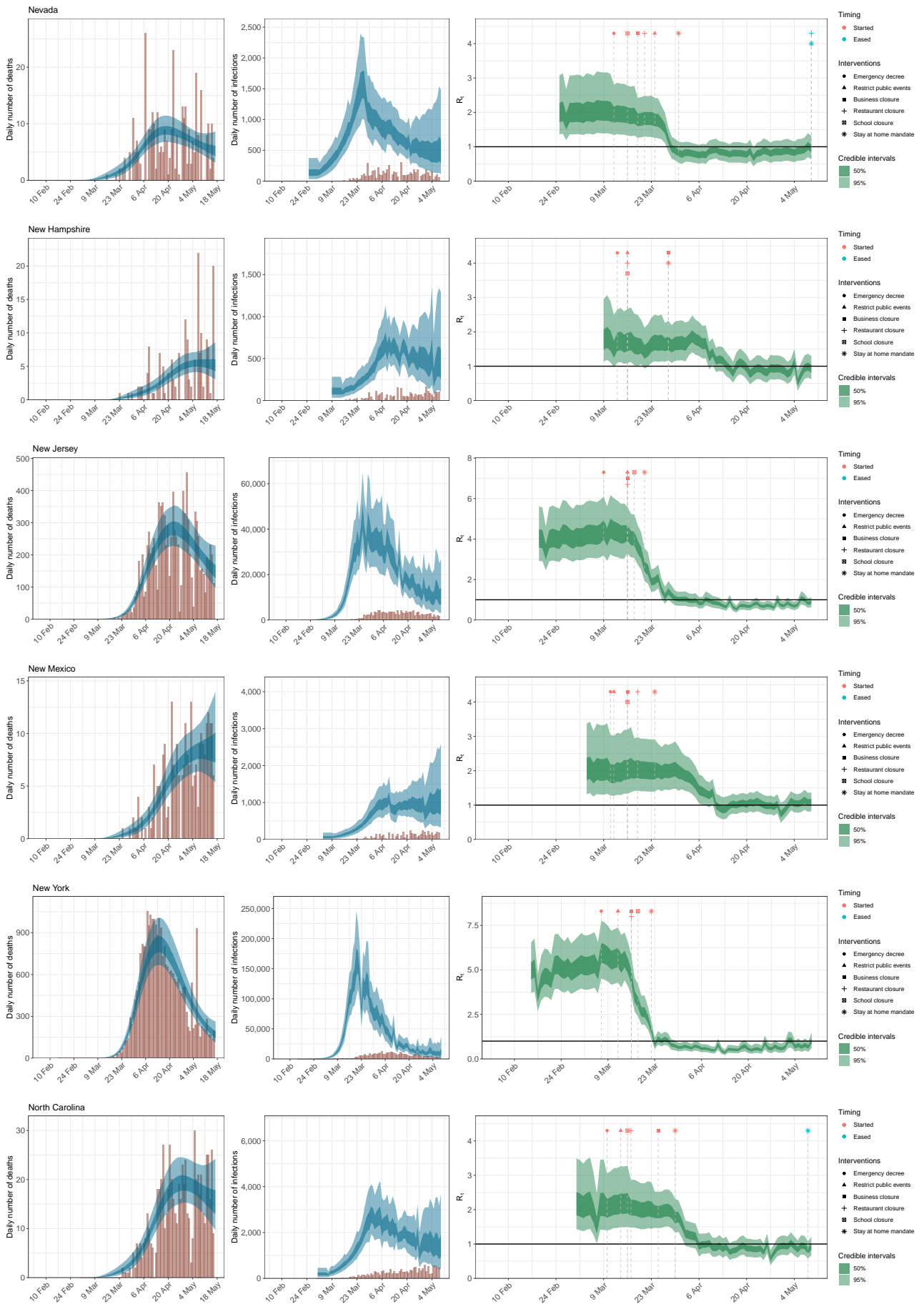


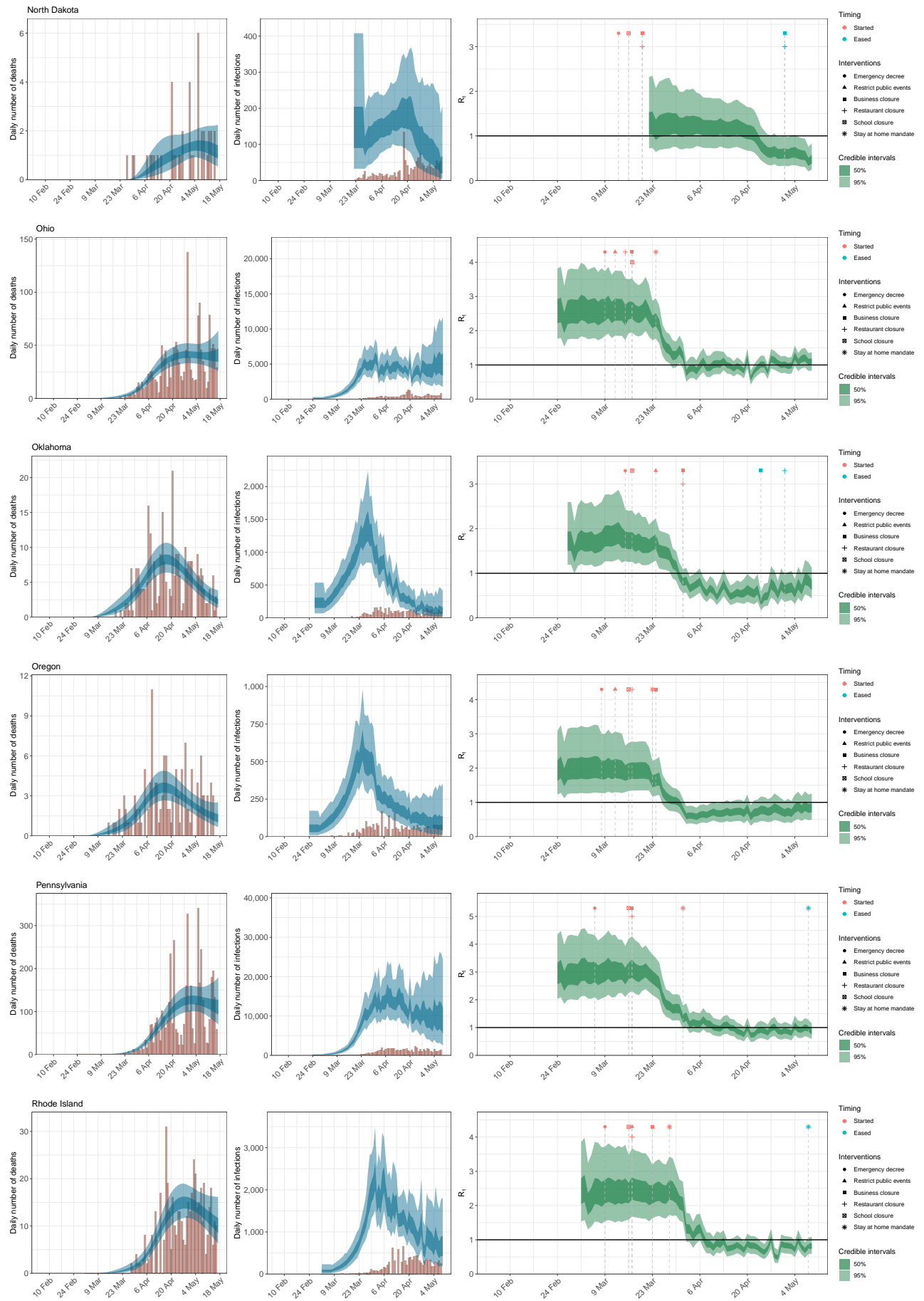


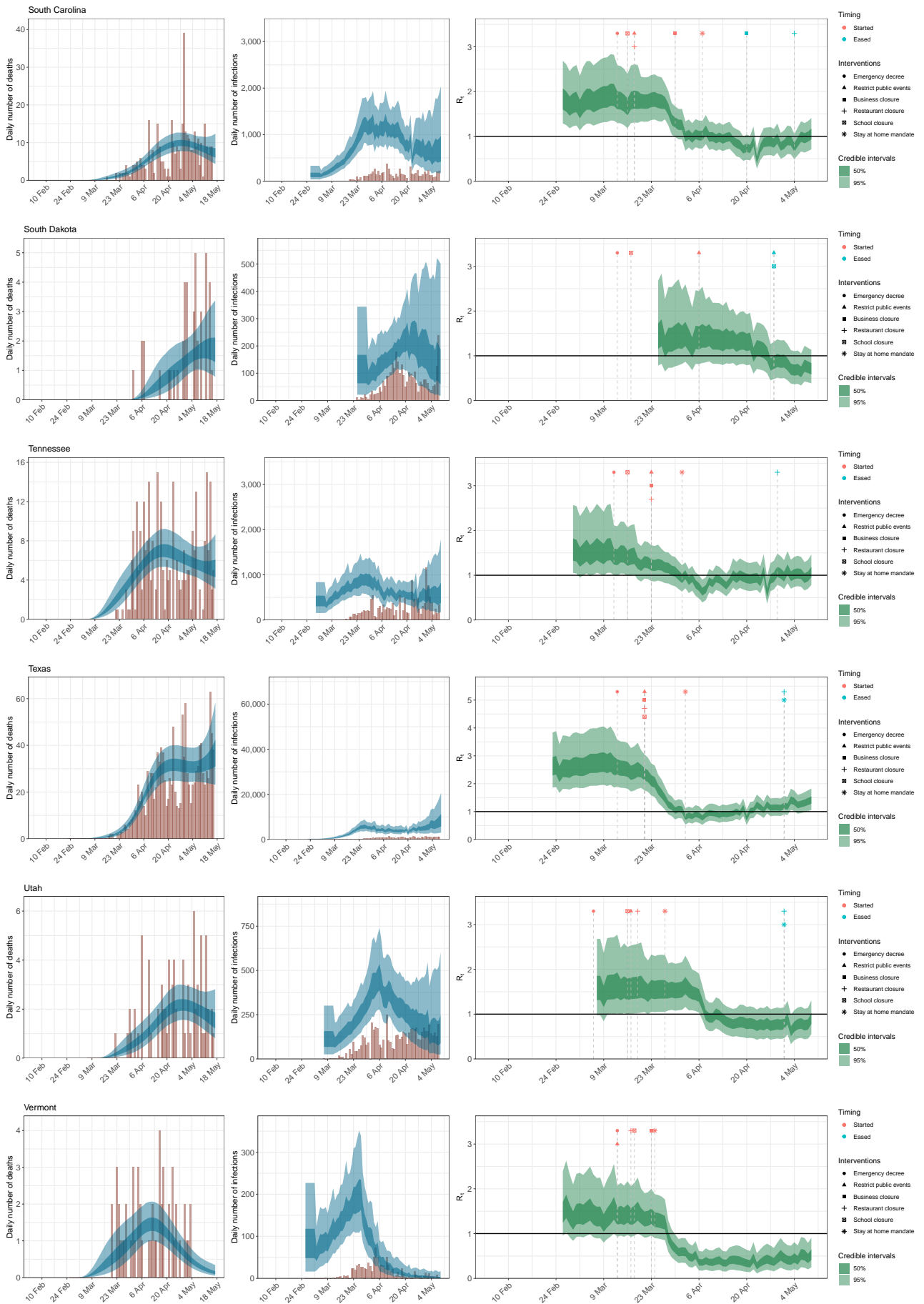


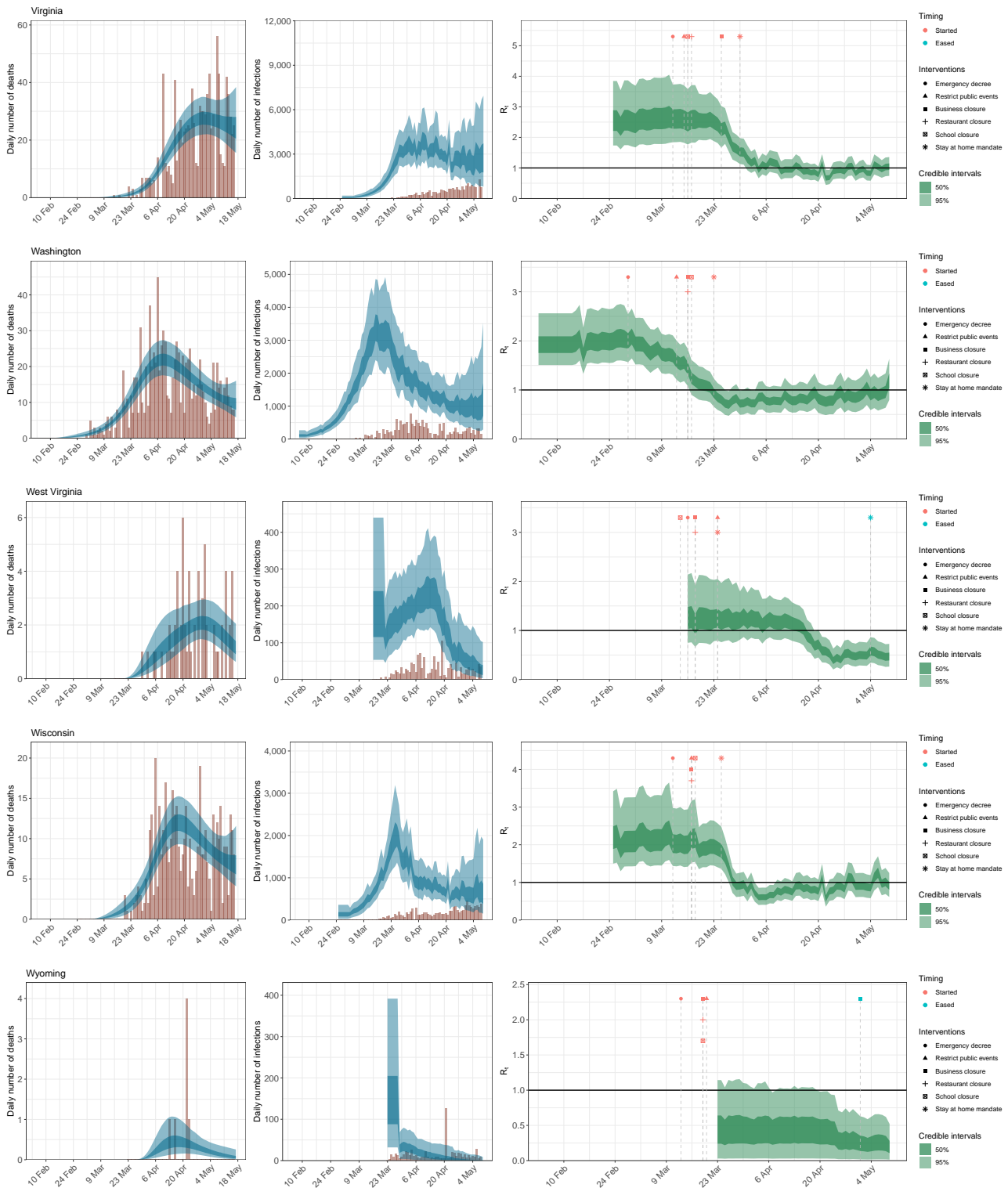












E Effective number of infectious individuals for all states

The effective number of infectious individuals, c^* , on a given day is calculated by weighing how infectious a previously infected individual is on a given day. The fully infectious average includes asymptomatic and symptomatic individuals. Estimates of the effective number of infectious individuals for all states can be found in Figure 13.

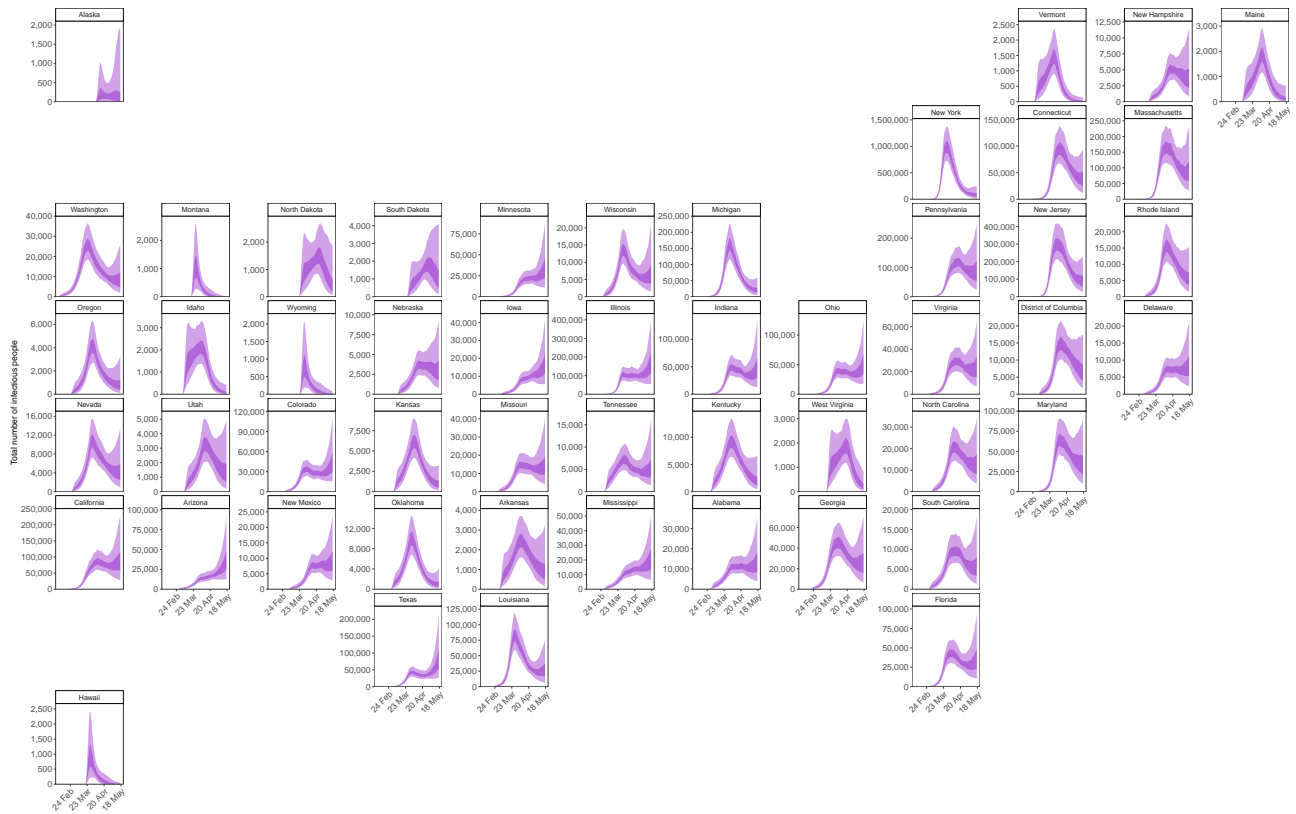


Figure 13: Estimates for the effective number of infectious individuals over time. The light purple region shows the 95% credible intervals and the dark purple region shows the 50% credible intervals.

To be more precise, the effective number of infectious individuals of infectious individuals, c^* , is calculated by first rescaling the generation distribution by its maximum, i.e. $g_\tau^* = \frac{g_\tau}{\max_t g_t}$. Based on (1), the number of infectious individuals is then calculated from the number of previously infected individuals, c , using the following:

$$c_{t,m}^* = \sum_{\tau=0}^{t-1} c_{\tau,m} g_{t-\tau}^*$$

where $c_{t,m}$ is the number of new infections on day t in state m . A plot of g_τ^* can be found in Figure 14.

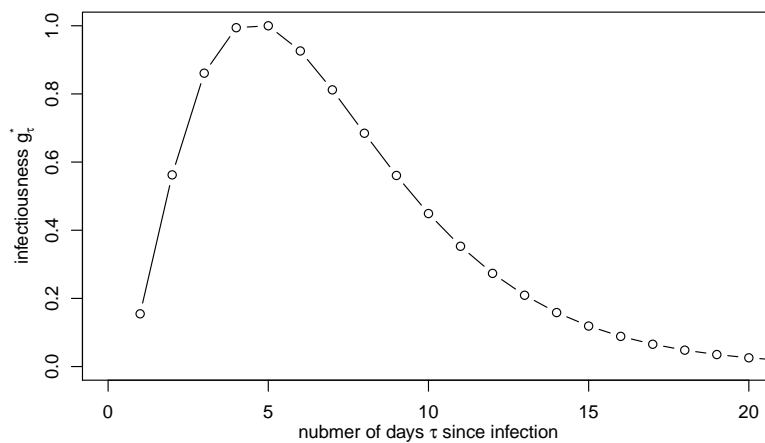


Figure 14: Infectiousness g_τ^* of an infected individual over time.

F Scenario results for all states

We show here state level scenario plots of an increase of mobility 20% and 40% of current levels.

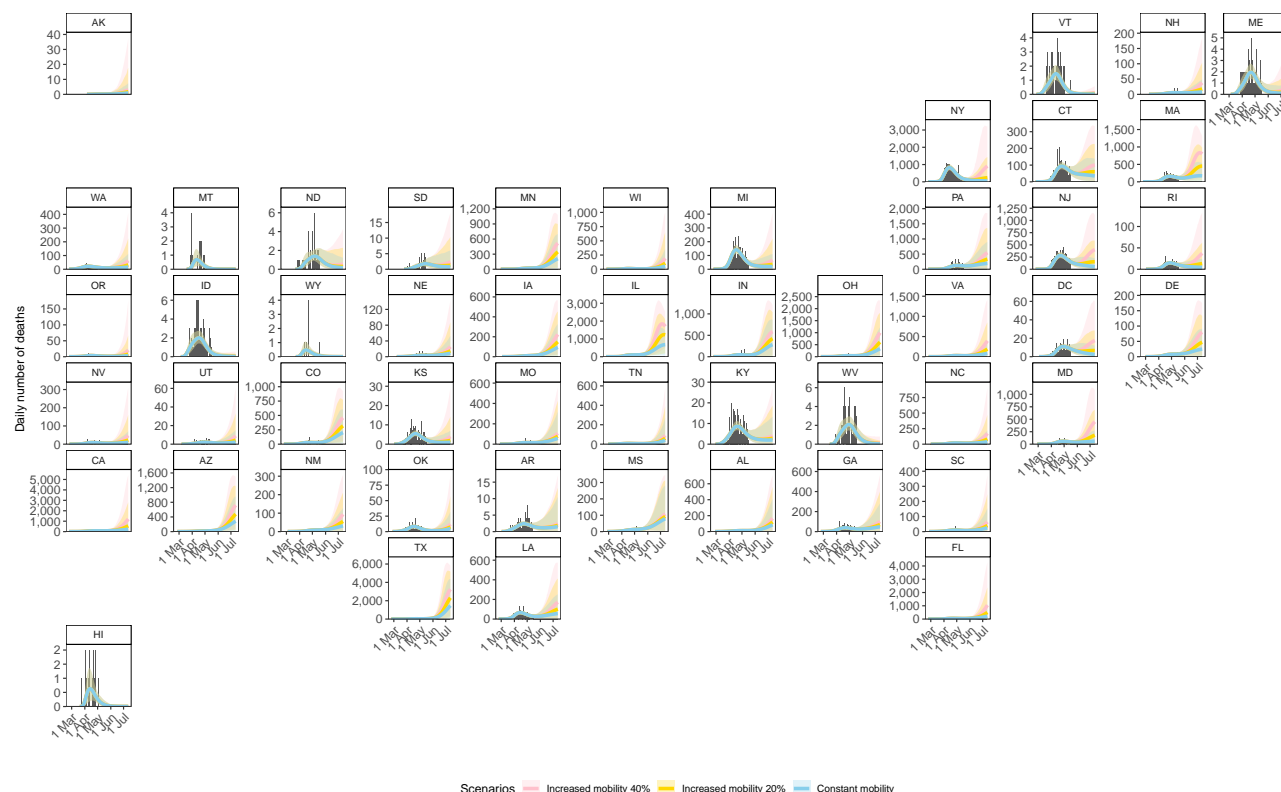


Figure 15: State-level scenario estimates for deaths. The blue ribbon shows the 95% credible intervals (CIs) for scenario (a) where mobility is kept constant at pre-lock down levels, the yellow ribbon shows the same CIs for scenario (b) where there is a 20% return to pre-epidemic mobility and scenario (c) where there is a 40% return to pre-epidemic.

G Sensitivity analysis to infection fatality ratio

Geographic-specific contact surveys are important for calculating the weighted IFR values according to the methods in [22, 23]. There is no large-scale cross-generational contact survey, similar to the polymod survey [19], implemented in the USA. Therefore, it was important to understand if the model was robust to changes in the underlying contact survey. We calculated the IFRs using three different contact matrices: UK, France and Netherlands. We believe that the USA is culturally closest to that UK out of those countries we had contact matrices for, but also considered France where we saw the greatest mixing of the elderly and the Netherlands which showed the *average* behaviour of the European studies used in [23]. We found that the IFR, calculated for each state using the three contact matrices, lay within the posterior of IFR in our model (Figure 16). We also noted that our results remained approximately constant when using the IFR calculated from the three different contact matrices as the mean of the prior IFR in our model, see Section 5.

Since we are using the same contact matrix across all the states, the differences in IFR are due to the population demographics and not due to differential contacts. The low IFR in Texas and Utah reflects the younger population there whereas the higher IFR in Florida and Maine is due to the older population. This is a limitation of our methods.

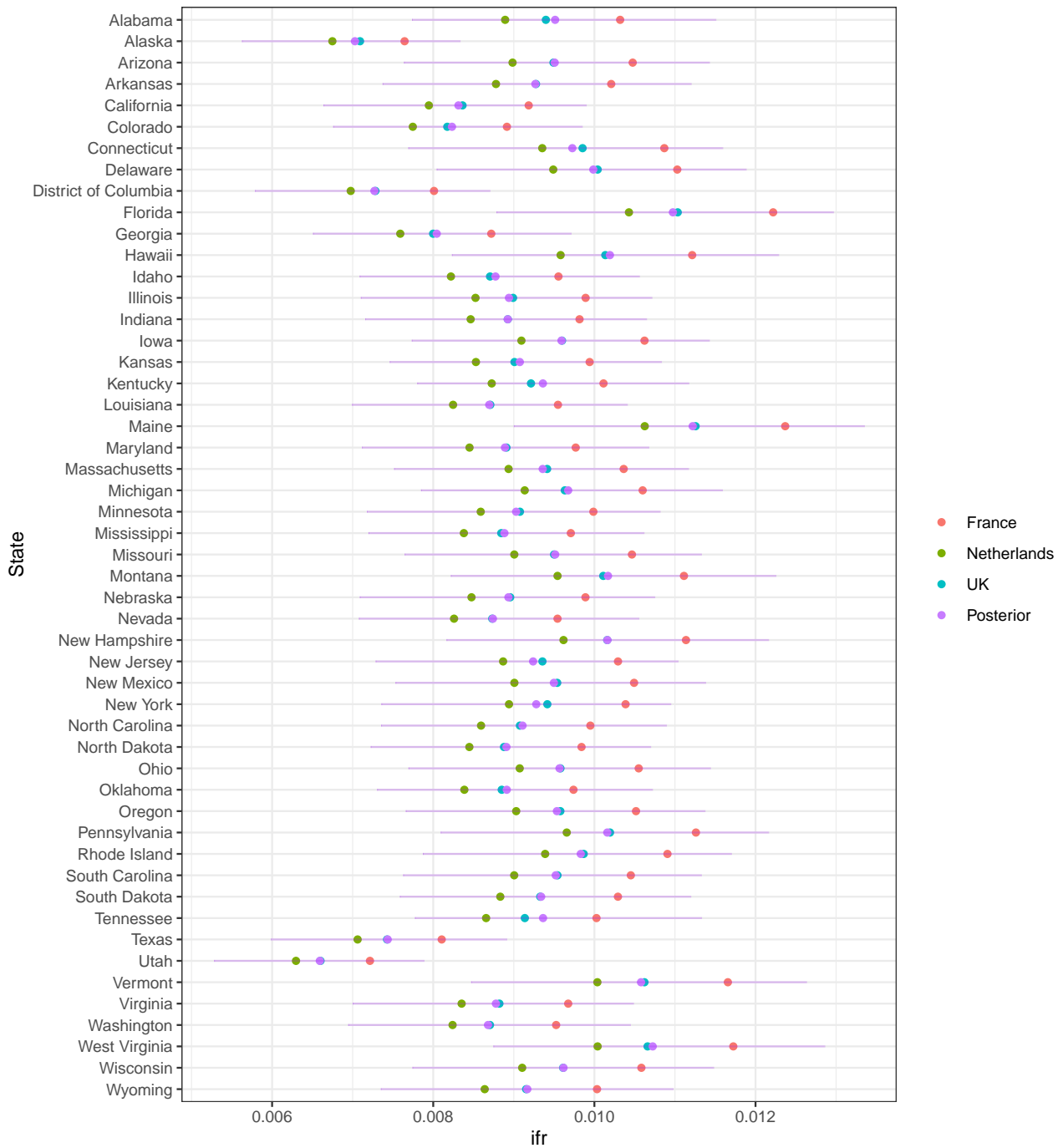


Figure 16: Sensitivity analysis for IFR. The red, green and blue dots show the IFR values calculated according to [22, 23] using the French, Dutch and and UK contact matrices respectively. The purple dot shows the mean of our posterior estimates for the IFR run using the UK contact matrix estimate and the purple error shows the 95% credible intervals of the distribution.